

# Learning with Calibration: Exploring Test-Time Computing of Spatio-Temporal Forecasting

Wei Chen, Yuxuan Liang\*

INTR & DSA Thrust, The Hong Kong University of Science and Technology (Guangzhou)

Spatio-temporal forecasting is crucial in many domains, such as transportation, meteorology, and energy. However, real-world scenarios frequently present challenges such as signal anomalies, noise, and distributional shifts. Existing solutions primarily enhance robustness by modifying network architectures or training procedures. Nevertheless, these approaches are computationally intensive and resource-demanding, especially for large-scale applications. In this paper, we explore a *novel test-time computing paradigm, namely learning with calibration, ST-TTC, for spatio-temporal forecasting*. Through learning with calibration, we aim to capture periodic structural biases arising from non-stationarity during the testing phase and perform real-time bias correction on predictions to improve accuracy. Specifically, we first introduce a spectral-domain calibrator with phase-amplitude modulation to mitigate periodic shift and then propose a flash updating mechanism with a streaming memory queue for efficient test-time computation. ST-TTC effectively bypasses complex training-stage techniques, offering an efficient and generalizable paradigm. Extensive experiments on real-world datasets demonstrate the effectiveness, universality, flexibility and efficiency of our proposed method.

**Repository:** <https://github.com/Onedean/ST-TTC> (Fully Open Source)

**Publish:** This work has been accepted by [NeurIPS 2025 \(Spotlight\)](#).

**Correspondence:** onedeanxxx@gmail.com, \*yuxliang@outlook.com

**Date:** May 31, 2025

## 1 Introduction

Spatio-temporal forecasting (STF) aims to predict the future state of dynamic systems from historical spatio-temporal observations and underpins many real-world applications, such as traffic flow forecasting (Guo et al., 2021), air quality forecasting (Nguyen et al., 2023), and energy consumption forecasting (Wang et al., 2019). Although spatio-temporal neural networks (Jin et al., 2023, 2024; Shao et al., 2024b), which couple spatial neural operators with temporal neural operators, have achieved remarkable progress on these tasks, their deployment in practical environments remains fraught with challenges. These observations, typically collected by sensors, are frequently corrupted by noise, outliers (*e.g.*, spikes or dropouts due to hardware failure) (Xu et al., 2024a), and more commonly, non-stationary distribution shifts arising from sensor aging and seasonal patterns (Wang et al., 2024d).

To enhance generalization and performance, prior work has focused primarily on out-of-distribution (OOD) learning for ST data during the training phase: designing architectures that resist perturbations (Ji et al., 2025; Ma et al., 2024; Wang et al., 2024a; Xia et al., 2023), augmenting training data with noise or adversarial examples (Bai et al., 2025; Liu et al., 2022; Zhang et al., 2023a), and introducing specialized loss functions or regularizers (Li et al., 2024b; Zhang et al., 2023b) to counteract distribution drift. However, these methods share fundamental limitations: they assume that the training data sufficiently captures all future target domain invariance, *a premise that is rarely valid in real-world settings*. Concurrently, an emerging paradigm of continual fine-tuning (Chen and Liang, 2025; Chen et al., 2021; Lee and Park, 2024; Wang et al., 2024b, 2023a,b) has become popular in spatio-temporal learning by continuously tuning the model to adapt to dynamic changes. Though promising, it still divides the target domain into multiple periods of training and testing and relies on period-specific training data to optimize model, *thereby failing in data-sparse scenarios*.

**Table 1** Formal comparison of different spatio-temporal learning paradigms for generalization from the perspective of data and learning.  $s$  denotes the source domain,  $t$  denotes the target domain,  $x$  and  $y$  denote the samples and labels sampled from  $\mathbf{X}$  and  $\mathbf{Y}$ , respectively. OOD learning expects inputs sampled from any environment  $e^* \sim \mathcal{E}$  to be valid, while others are only optimized for the current training or test environment  $e$ . In particular, continual fine-tuning divides the target domain into multiple stages and optimizes for a specific stage  $\tau$  environment  $e^\tau$ .  $\times$  means not involved.

Setting	Example Works	Data Perspective		Learning Perspective	
		Source	Target	Train-Time	Test-Time
OOD Learning	STONE (Wang et al., 2024a), CaST (Xia et al., 2023)	$(\mathbf{X}^s, \mathbf{Y}^s)$	$\times$	$\min_{f_\theta} \max_{e^* \in \mathcal{E}} \mathbb{E}_{(x,y) \sim P(\mathbf{X}^s, \mathbf{Y}^s   e^*)} [L(f_\theta(x), y)]$	$\times$
Continual Fine-Tuning	EAC (Chen and Liang, 2025), TrafficStream (Chen et al., 2021)	$\times$	$(\mathbf{X}^t, \mathbf{Y}^t)$	$\min_{f_{\theta^\tau}} \mathbb{E}_{(x,y) \sim P(\mathbf{X}^t, \mathbf{Y}^t   e^\tau)} [L(f_{\theta^\tau}(x), y)]$	$\times$
Test-Time Training	TTT-ST (Chen et al., 2024)	$\mathbf{X}^s$	$\mathbf{X}^t$	$\min_{f_\theta} \mathbb{E}_{(\tilde{x}, x) \sim P(\mathbf{X}^s   e)} [L(f_\theta(\tilde{x}), x)]$	$\min_{f_\theta} \mathbb{E}_{(\tilde{x}, x) \sim P(\mathbf{X}^t   e)} [L(f_\theta(\tilde{x}), x)]$
Online Continual Learning	DOST (Wang et al., 2024c)	$\times$	$\mathbf{X}^t$	$\times$	$\min_{f_{\theta(\delta)}} \mathbb{E}_{(x,y) \sim P(\mathbf{X}^t   e)} [L(f_{\theta(\delta)}(x), y)]$
Test-Time Computing	ST-TTC (Our)	$\times$	$\mathbf{X}^t$	$\times$	$\min_{g_\theta} \mathbb{E}_{(x,y) \sim P(\mathbf{X}^t   e)} [L(g_\theta(f_\theta(x)), y)]$

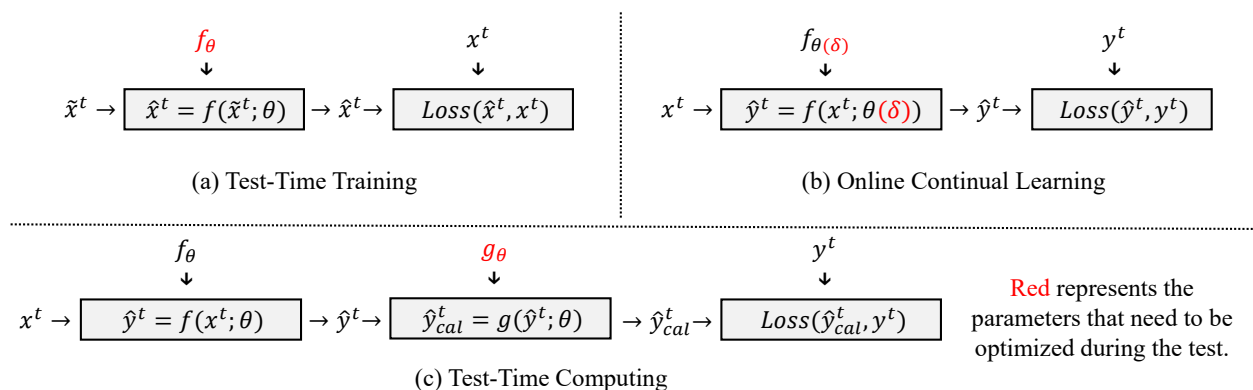


**Figure 1** Conceptual visualization comparison of different spatio-temporal learning paradigms under test environment. (a) *Test-Time Training* requires the use of additional pretext tasks in the training and test phases to optimize the self-supervision head or the overall model parameters  $f_\theta$ . (b) *Online Continual Learning*, by optimizing some internal parameters  $f_{\theta(\delta)}$  of the model, requires additional modifications to the internal architecture of the network. Our (c) *Test-Time Computing* method only requires a lightweight calibrator  $g_\theta$ , which is a seamless and lightweight plug-and-play module.

Recently, leveraging test-time information has attracted widespread attention for its ability to significantly improve language model performance on complex reasoning tasks (Akyürek et al., 2024; Snell et al., 2025). In computer vision, this concept has already been extensively developed: test-time training (TTT) was first introduced by (Sun et al., 2020), which defines an auxiliary self-supervised task applied to both training and test samples to better balance bias and variance (Gandelsman et al., 2022). A similar idea was adapted to spatio-temporal forecasting in TTT-ST (Chen et al., 2024). Unlike language and vision settings—where obtaining ground-truth labels for test samples at inference time is nearly impossible—STF benefits from label autocorrelation (Cressie and Wikle, 2011): each observation strongly depends on its predecessor, and training instances are constructed from sliding windows, which provide access to historical samples and their true labels. Moreover, this property makes STF also require timeliness (Shao et al., 2024a), that is, the additional computing time during inference must be less than the window-stride interval. A recent STF method, DOST (Wang et al., 2024c), explores online continual learning, which initially explored this direction. It uses historical test sample labels to dynamically adapt the modified model architecture. *Though promising, these approaches typically involve complex self-supervised tasks or structural adaptations and still fall short of the timeliness demands of STF.*

To address this gap, we propose Test-Time Computing of Spatio-Temporal Forecasting (ST-TTC), an attractive complementary paradigm. ST-TTC achieves learning with calibration by iteratively leveraging available test information during inference, enabling seamless integration with diverse models. This adapts the model to

evolving spatio-temporal patterns, thereby calibrating predictions. Our principal insight is that performance degradation during test time is primarily driven by non-stationary distributional shifts stemming from progressive periodic biases. Therefore, we propose a spectral domain calibrator. This involves appending a lightweight module, operating in the frequency domain, subsequent to the backbone network. This module calibrates biases by learning minor, node-specific amplitude and phase correction factors. Furthermore, a flash gradient updating mechanism with a streaming memory queue, ensures universal, rapid, and resource-efficient test-time computing. Table 1 provides a formal comparison of our method against existing learning paradigms, and Figure 1 offers a conceptual visualization of learning with test domain. In summary, our contributions are:

- We propose a novel test-time computing paradigm of spatio-temporal forecasting, termed ST-TTC .
- We systematically explore the goals and means of achieving this paradigm. Concretely, we introduce a spectral domain calibrator with phase-amplitude modulation to mitigate periodic shift and present a flash updating mechanism with a streaming memory queue for efficient test-time computation.
- Experimental results on real-world spatio-temporal datasets in different fields, scenarios, and learning paradigms demonstrate the effectiveness and universality of ST-TTC .

## 2 Related Work

**Spatio-Temporal Forecasting.** Spatio-temporal sequences can be regarded as spatially extended multivariate time series. Although one can trivially apply multivariate forecasting methods (Biller and Nelson, 2003; Box and Pierce, 1970; Nie et al., 2023; Zeng et al., 2023) independently at each location, such decoupling of spatial and temporal dependencies invariably yields suboptimal results (Shao et al., 2024b). Classical spatio-temporal forecasting method instead relies on shallow models or spatio-temporal kernels, including feature-based methods (Ohashi and Torgo, 2012; Zheng et al., 2015), state space models (Bahadori et al., 2014; Cliff and Ord, 1975; Pfeifer and Deutsch, 1980), and Gaussian process models (Flaxman, 2015; Senanayake et al., 2016). Unfortunately, the overall nonlinearity of these models is limited, and the high complexity of computation and storage further hinders the availability of massive training instances (Shi and Yeung, 2018). In recent years, spatio-temporal neural networks (Jin et al., 2023, 2024; Kumar et al., 2024) have been widely adopted to learn the complex dynamics of such systems. Early work concentrated on devising neural operators to extract spatial or temporal correlation (Fang et al., 2025; Liu et al., 2023a; Shao et al., 2022b; Wu et al., 2019; Yu et al., 2018) and on designing fusion architectures to integrate them (Cini et al., 2023; Deng et al., 2024; Guo et al., 2019; Li et al., 2018; Oreshkin et al., 2021). More recent efforts have explored domain-invariant representation learning (Ma et al., 2024; Zhou et al., 2024, 2023) and continual model adaptation (Chen and Liang, 2025; Kieu et al., 2024; Chen et al., 2021; Yi et al., 2024) to better accommodate unseen environmental shifts. *However, these methods still depend exclusively on offline training data and thus cannot deliver truly timely and effective adaptation in real settings.*

**Test-Time Computing.** Test-time computation is inspired by the human cognition (Kahneman, 2011), in which additional computational effort is allocated during inference to improve task performance. This insight has recently driven considerable interest in the nature language process community, fueled by the success of reasoning-augmented language models (*e.g.*, o1 (Jaech et al., 2024) and r1 (Guo et al., 2025)) that activate and adapt internal computations at test time via supervised fine-tuning or reinforcement learning (RL) (Zhang et al., 2025). While the generalization properties of RL-based adaptation remain debated (Yue et al., 2025), the notion of supervised learning on unlabeled test data dates back to “transductive learning” (Gammerman et al., 1998) in the 1990s and has demonstrated empirical benefits (Bottou and Vapnik, 1992; Vapnik, 1999). In the computer vision domain, this idea was formalized as Test-Time Training (Sun et al., 2020), which attaches an auxiliary self-supervised head to enable online adaptation to each test instance—a paradigm subsequently generalized as test-time adaptation (Jang et al., 2023; Liang et al., 2025; Wang et al., 2021, 2022). However, spatio-temporal forecasting has seen limited exploration of such techniques. TTT-ST (Chen et al., 2024) applies TTT-style auxiliary objectives during training and continues to update at inference, and DOST (Wang et al., 2024c) further incorporates dynamic learning mechanisms within modified model architectures for test-time updates. In addition, some methods (Guo et al., 2024; Zhang et al., 2023c) are conceptually close to ours, such as CompFormer (Zhang et al., 2023c), which proposes a test-time compensated representation learning framework, but still requires access to additional training data. *Notably, we formalize the test-time computing of spatio-temporal forecasting, and propose a unified learning-with-calibration framework that is*

general, lightweight, efficient, and effective for STF at test-time.

For more related work, we provide a more detailed introduction in Appendix A.

### 3 Preliminaries

**Problem Definition.** Let  $x \in \mathbb{R}^{T \times C}$  denote the multivariate time series recorded at each location sensor, capturing the dynamic observations of  $C$  measured features in  $T$  consecutive time steps. Stacking these sequences for all  $N$  locations yields the spatio-temporal tensor  $X \in \mathbb{R}^{N \times T \times C}$ . Given historical observations  $X^h \in \mathbb{R}^{N \times T^h \times C}$  (and an optional spatial correlation graph  $\mathcal{G}$  representing the spatial relationships of  $N$  locations), spatio-temporal forecasting aims to learn a mapping  $f_\theta : (X^h, \mathcal{G}) \mapsto X^f \in \mathbb{R}^{N \times T^f \times C}$ , where  $X^f$  is the signal for the next  $T^f$  time steps. In practice, according to (Li et al., 2018; Shao et al., 2024b), the feature to be predicted is usually only the target variable.

**Scenario Definition.** In deep learning systems, batch-based testing is typically employed to exploit parallelism. In real-world deployment, however, predictions must be produced for each incoming time-step sample—*i.e.*, with batch size  $B$  set to 1. At time index  $t$ , once the new sliding-window input  $X_t \in \mathbb{R}^{N \times T^h \times C}$  arrives, the true labels for all test samples before time index  $t - T^h - T^f + 1$  become available. Thus, test-time computing of spatio-temporal forecasting can leverage this accumulated historical information to enhance the accuracy of the current prediction, while ensuring that any additional computation latency remains below a threshold defined by the sliding-window stride.

## 4 Methodology

Our test-time computing framework of spatio-temporal forecasting (ST-TTC) integrates two synergistic components: 1) a spectral domain calibrator with phase-amplitude modulation; and 2) a flash gradient update mechanism with streaming memory queue. In this section, we introduce these two key components, respectively, from the perspective of what is computed and how it is computed.

### 4.1 What to Compute? Spectral Domain Calibrator with Phase-Amplitude Modulation

**Motivation.** Spatio-temporal data, such as traffic flow and air quality, often exhibit periodic patterns (*e.g.*, daily or weekly cycles). However, in real-world deployments, these patterns are not stationary; they are dynamically influenced by various internal and external factors (Wang et al., 2024e). Such influences lead to non-stationarities manifesting as fluctuations in amplitude (*e.g.*, increased or decreased traffic peaks due to seasonal changes) or phase shifts (*e.g.*, peak hours are advanced or delayed due to traffic congestion). Pre-training models typically fit fixed periodic patterns during training, which makes them vulnerable to performance degradation under such persistent dynamic changes during inference (Wang et al., 2024d). Therefore, we argue that *the goal of test-time computation is: how to design an effective calibrator that can efficiently capture such gradual systematic bias from the pattern to correct the prediction errors caused by non-stationarity, while avoiding overfitting to random noise?*

**Key Challenges.** While correction in the time domain is possible (Guo et al., 2024; Zhang et al., 2023c), it often requires extensive parameterization, leading to increased model complexity and limited ability to capture evolving periodic structures. Moreover, the coupled structural and branching modules (Chen et al., 2024; Wang et al., 2024c) are prone to overfitting the random noise in the spatio-temporal evolution. To address this, we propose calibration in the spectral domain, where periodic variations are more transparently expressed as changes in the amplitude and phase of specific frequency components. Spectral correction offers a potentially more direct and robust solution. However, this introduces two main challenges: ❶ the degree of non-stationarity varies across spatial nodes; and ❷ full-spectrum parameterization is computationally expensive. *The core problem thus becomes how to design a lightweight, spatial-aware calibrator.*

**Implementation Details.** To this end, we formally introduce the *spectral domain calibrator (SD-Calibrator)*, which is a lightweight plug-and-play module that performs spectral domain calibration on the time domain

prediction results of the pre-trained model, aiming to achieve efficient test-time computation for spatio-temporal forecasting. Specifically, it can be divided into three steps:

- *Spatial-aware Decomposition.* To ensure spatial awareness, we apply a real-to-complex fast Fourier transform (rFFT) along the time dimension of the backbone model’s prediction  $\hat{y} \in \mathbb{R}^{B \times N \times T}$ , separately for each spatial node. This yields the frequency spectrum:  $Y_f = \text{rFFT}(\hat{y}) \in \mathbb{C}^{B \times N \times M}$ , where  $M = \frac{T}{2} + 1$  is the number of unique frequency bins for real-valued signals. Then, we decompose  $Y_f$  into its amplitude  $A = |Y_f| \in \mathbb{R}^{B \times N \times M}$  and phase  $P = \angle Y_f \in \mathbb{R}^{B \times N \times M}$ .
- *Group-wise Modulation.* To ensure lightweight and balanced spectrum expression, we divide the  $M$  frequency bins into  $G$  contiguous groups of size  $\lfloor M/G \rfloor$ , and learn per-group, per-node amplitude and phase offsets  $\lambda^\alpha \in \mathbb{R}^{G \times N \times 1}$ ,  $\lambda^\phi \in \mathbb{R}^{G \times N \times 1}$  (Note: Both  $\lambda^\alpha$  and  $\lambda^\phi$  are initialized to 0 to avoid incorrect calibration of predictions before learning). For each group  $g \in \{1, \dots, G\}$ , we apply  $A'_g = A_g \odot (1 + \lambda_g^\alpha)$ ,  $P'_g = P_g + \lambda_g^\phi$ , and reconstruct the spectrum as  $Y'_f = \bigcup_{g=1}^G A'_g \odot e^{(j P'_g)}$ .
- *Inverse Transform.* Finally, the calibrated time-domain signal is obtained by Inverser rFFT  $\hat{y}_{cal} = \text{irFFT}(Y'_f) \in \mathbb{R}^{B \times N \times T}$ , along the frequency dimension.

For clarity, we provide a Algorithm workflow 1 and Pytorch-Style Pseudocode 1 in Appendix C.1.

**Complexity Analysis.** The full-spectrum parameterization learns independent amplitude and phase offsets for each of the  $M = T/2 + 1$  frequency bins and  $N$  nodes, totaling  $2NM$  parameters. In contrast, our  $G$ -group design learns only  $2NG$  parameters. Since  $G$  is a constant and  $M$  grows linearly with  $T$ ,  $G \ll M$  is usually the case. For large-scale long-term scenario, this significantly reduces memory footprint and gradient update cost while retaining interpretable per-band calibration.

**Theoretical Analysis.** We also provide a theoretical approximate bound on the output perturbation induced by the *SD-Calibrator*, ensuring controlled deviation from the original prediction to prevent overfitting (Please refer to Theorem 1 and the proof in Appendix B).

## 4.2 How to Compute ? Flash Gradient Update with Streaming Memory Queue

**Motivation.** The *SD-Calibrator* provides an effective mechanism for output correction. To accommodate the dynamic nature of spatio-temporal data, its parameters  $(\lambda^\alpha, \lambda^\phi)$  must be continuously updated during inference. Fortunately, as we discussed above, due to the streaming nature of spatio-temporal data, unlike Visual and textual tasks, we have access to the true labels of historical samples. However, simply accumulating all historical data for updates is not feasible due to the increasing computational load and memory usage. Therefore, we argue that *the key to test-time computation is: How to design an efficient data selection and learning mechanism that leverages appropriate historical information to tuning the SD-Calibrator without incurring a lot of computational overhead?*

**Key Challenges.** Although retrieving similar sequences from historical training databases can partially compensate for prediction errors (Zhang et al., 2023c), this assumption is unrealistic, as only test-time information is available in our scenario. Moreover, selectively storing historical test samples via memory bank primarily serves to mitigate catastrophic forgetting in the backbone model (Wang et al., 2024c), which misaligns with the learning objective of our *SD-calibrator*. To address this, we propose freezing the backbone and updating only the calibrator using recent test samples for efficient test-time computing. However, this strategy introduces two critical challenges: ❶ recent studies (Lau et al., 2025) have shown that real-time updates may cause information leakage; and ❷ excessive updates can lead to overfitting of the calibration parameters and increased computational burden. *The core problem thus becomes how to design a efficient calibration parameter learning mechanism without information leakage.*

**Implementation Details.** To address these challenges, we introduce the *flash gradient update* strategy coupled with a *streaming memory queue*. The process is as follows:

- *Streaming Memory Queue.* We maintain a first-in, first-out (FIFO) queue, denoted as  $\mathcal{Q}$ , with a maximum size equal to the prediction horizon  $T^f$ . For each incoming test instance  $t$ , after making a prediction, we store the input-label pair  $(X_t, Y_t)$  into  $\mathcal{Q}$  (Here is for engineering convenience. In real deployment, data points can be merged at each step to form the true label). Once  $\mathcal{Q}$  is full, for every new test sample

$(X_n, Y_n)$  added, the oldest sample pair  $(X_o, Y_o)$  is dequeued. This dequeued sample  $(X_o, Y_o)$  is then used for the gradient update, thus avoiding the information leakage.

- *Flash Gradient Update.* Once we have  $(X_o, Y_o)$ , we first obtain the backbone model’s prediction for the historical input:  $\hat{Y}_o^b = f_\theta(X_o)$  (note: the backbone model weights  $f_\theta$  are frozen). Then, the *SD-Calibrator*  $g_\theta$  processes this prediction:  $\hat{Y}_o^{cal} = g_\theta(\hat{Y}_o^b)$ . The loss function between the calibrated prediction  $\hat{Y}_o^{cal}$  and the true historical label  $Y_o$  is calculated, and only a single gradient descent step is performed to update the parameters of the *SD-Calibrator*:  $\lambda \leftarrow \lambda - \eta \nabla_\lambda L$ . For the next input sample  $X_t$ , the updated *SD-Calibrator* is used for prediction. Using this single-sample single-step gradient descent strategy, we achieve lightning-fast parameter updates.

For clarity, we provide a Algorithm workflow 2 and Pytorch-Style Pseudocode 2 in Appendix C.2.

**Complexity Analysis.** The primary focus here is the time complexity. The *Streaming Memory Queue* itself has an  $\mathcal{O}(1)$  time complexity for enqueue and dequeue operations. The *Lightning Gradient Update* is performed only once for each incoming test sample. Each update involves: 1). Forward propagation of the backbone and calibrator (dominated by the computational cost  $\mathcal{O}(NT \log T)$  of rFFT and irFFT) 2). Backward propagation of the calibrator (dominated by parameter cost  $\mathcal{O}(NG)$ ).

**Theoretical Analysis.** We also show that this single update step leads to a controlled adjustment, ensuring that the calibrator makes progress on the newest sample it’s trained on, without causing erratic behavior, under standard assumptions. (Please refer to Proposition 2 in Appendix B).

## 5 Experiments

In this section, we conduct extensive experiments to answer the following research questions (RQs):

- **RQ1:** Can ST-TTC have a consistent improvement on various types of models and datasets? Can ST-TTC outperform previous learning methods that leverage test data? (*Effectiveness*)
- **RQ2:** Can ST-TTC effective in various real-world scenarios, including few-shot learning, long-term forecasting, and large-scale forecasting? (*Universality*)
- **RQ3:** Can ST-TTC further enhance the performance of existing learning paradigms that utilize training data, such as OOD Learning and continual learning? (*Flexibility*)
- **RQ4:** How does ST-TTC work? Which components or strategies are crucial? Are these components or strategies sensitive to parameters or design? (*Mechanism & Robustness*)
- **RQ5:** What is the time and parameter cost of ST-TTC during test-time computation, and how does it compare to other advanced methods? (*Efficiency & Lightweight*)

### 5.1 Experimental Setup

**Datasets.** We employ publicly available benchmark datasets widely used in the literature to cover typical spatio-temporal forecasting scenarios in the traffic domain (*PEMS-03, PEMS-04, PEMS-07, PEMS-08* (Song et al., 2020)), the meteorological domain (*KnowAir* (Wang et al., 2020)), and the energy domain (*UrbanEV* (Li et al., 2025)). In addition, we also leverage the traffic-speed benchmark *METR-LA* (Li et al., 2018), the large-scale spatio-temporal benchmark *LargeST* (Liu et al., 2023b), and dynamic-stream benchmarks (*Energy-Stream, Air-Stream, PEMS-Stream* (Chen and Liang, 2025)) to assess our methods across varied settings and learning paradigms. Unless otherwise specified, all datasets are chronologically split into training, validation and test sets in a 6 : 2 : 2 ratio. For more detailed description of each dataset, please see the Appendix D.1.

**Baseline.** For the default evaluation, we cover various widely used spatio-temporal backbones, which can be divided into three categories: (1) Transformer-based: *STAEformer* (Liu et al., 2023a) and *STTN* (Xu et al., 2020); (2) Graph-based: *GWNet* (Wu et al., 2019) and *STGCN* (Yu et al., 2018); (3) MLP-based: *STID* (Shao et al., 2022b) and *ST-Norm* (Deng et al., 2021). For the baselines that leverage test information, we cover three types: (1) popular test-time adaptation methods in vision: *TTT-MAE* (Gandelsman et al., 2022) and *TENT* (Wang et al., 2021); (2) Online time series forecasting methods: *OnlineTCN* (Zinkevich, 2003), *FSNet* (Pham et al., 2023) and *OneNet* (Wen et al., 2023); (3) Comparable online spatio-temporal

forecasting methods: *CompFormer* (Zhang et al., 2023c) and *DOST* (Wang et al., 2024c). For the baselines on large-scale benchmarks, we use the efficient *PatchSTG* (Fang et al., 2025) as the backbone. For the baseline of OOD learning scenarios, we use the advanced *STONE* (Wang et al., 2024a) as the default method. For the continual learning scenario, we use *EAC* (Chen and Liang, 2025) and *STKEC* (Wang et al., 2023a) as the default methods. We follow the default parameter settings of the models for all scenarios according to the corresponding literature. For details of each method, see Appendix D.2.

**Protocol.** Following prior benchmarks (Shao et al., 2024b), we employ a 12-to-12 forecasting protocol—using the previous 12 time steps to predict the next 12 steps and their mean—evaluated with mean absolute error (MAE), root mean square error (RMSE), and mean absolute percentage error (MAPE). For simplicity, all experiments share the same hyperparameters of our ST-TTC : the calibration module learning rate  $lr$  is set to  $1e-4$ , the memory-queue sample count  $n$  used for updating is 1, and the number of groups  $m$  to 4. To ensure fairness, each experiment is repeated five times, with results reported as mean  $\pm$  standard deviation (denoted in gray  $\pm$ ). More protocol details, see Appendix D.3.

## 5.2 Effectiveness Study (RQ1)

**Consistent Effectiveness.** Table 2 presents the results of our method for 12-step future prediction across six models on six public datasets. The  $\times$  column denotes the results of standard testing, while the  $\checkmark$  column indicates results obtained with our proposed ST-TTC approach. The best results in the  $\times$  and  $\checkmark$  columns are highlighted in bold blue and pink fonts, respectively. We also compute the relative improvement, denoted by the  $\Delta$  column. Based on these results, we make the following observations: ① The application of our test-time computation method, ST-TTC , consistently yields performance gains across various backbone architectures and dataset combinations. ② From a model-centric perspective, our approach can further enhance the performance of even the top-performing methods across different metrics and datasets. ③ From a data-centric perspective, *UrbanEV* shows more significant relative improvement, likely due to its more pronounced distribution shift.

**Table 2** Performance comparison of different models w/ and w/o ST-TTC on common benchmarks.

Models	Transformer-based						Graph-based						MLP-based						
	<i>STAEformer</i> (Liu et al., 2023a)		<i>STTN</i> (Xu et al., 2020)				<i>GWNNet</i> (Wu et al., 2019)		<i>STGCN</i> (Yu et al., 2018)				<i>STID</i> (Shao et al., 2022b)		<i>ST-Norm</i> (Deng et al., 2021)				
w/ ST-TTC	$\times$	$\checkmark$	$\Delta$ (%)	$\times$	$\checkmark$	$\Delta$ (%)	$\times$	$\checkmark$	$\Delta$ (%)	$\times$	$\checkmark$	$\Delta$ (%)	$\times$	$\checkmark$	$\Delta$ (%)	$\times$	$\checkmark$	$\Delta$ (%)	
<i>PEMS-03</i>	MAE	17.00 $\pm$ 0.16	16.75 $\pm$ 0.14	$\downarrow$ 1.47	18.12 $\pm$ 0.53	17.88 $\pm$ 0.50	$\downarrow$ 1.32	16.73 $\pm$ 0.41	16.42 $\pm$ 0.19	$\downarrow$ 1.85	18.41 $\pm$ 0.35	18.08 $\pm$ 0.35	$\downarrow$ 1.79	17.48 $\pm$ 0.02	17.29 $\pm$ 0.01	$\downarrow$ 1.09	17.27 $\pm$ 0.13	17.03 $\pm$ 0.12	$\downarrow$ 1.39
	RMSE	29.98 $\pm$ 0.59	29.48 $\pm$ 0.58	$\downarrow$ 1.67	31.02 $\pm$ 1.55	30.48 $\pm$ 1.37	$\downarrow$ 1.74	28.48 $\pm$ 0.48	27.90 $\pm$ 0.13	$\downarrow$ 2.04	31.74 $\pm$ 0.94	31.10 $\pm$ 0.86	$\downarrow$ 2.02	29.10 $\pm$ 0.22	28.74 $\pm$ 0.21	$\downarrow$ 1.24	29.28 $\pm$ 0.20	28.71 $\pm$ 0.14	$\downarrow$ 1.95
	MAPE(%)	15.82 $\pm$ 0.22	15.82 $\pm$ 0.20	$\downarrow$ 0.00	18.43 $\pm$ 1.19	18.01 $\pm$ 1.06	$\downarrow$ 2.28	16.70 $\pm$ 0.60	16.49 $\pm$ 0.30	$\downarrow$ 1.26	18.90 $\pm$ 0.78	18.68 $\pm$ 0.44	$\downarrow$ 1.16	17.50 $\pm$ 0.12	17.39 $\pm$ 0.01	$\downarrow$ 0.63	17.20 $\pm$ 0.82	16.92 $\pm$ 0.52	$\downarrow$ 1.63
<i>PEMS-04</i>	MAE	19.48 $\pm$ 0.05	19.33 $\pm$ 0.06	$\downarrow$ 0.77	20.63 $\pm$ 0.03	20.48 $\pm$ 0.03	$\downarrow$ 0.73	20.57 $\pm$ 0.37	20.49 $\pm$ 0.39	$\downarrow$ 0.39	20.70 $\pm$ 0.14	20.57 $\pm$ 0.12	$\downarrow$ 0.63	19.97 $\pm$ 0.07	19.86 $\pm$ 0.08	$\downarrow$ 0.55	20.22 $\pm$ 0.10	20.08 $\pm$ 0.09	$\downarrow$ 0.69
	RMSE	32.58 $\pm$ 0.39	32.31 $\pm$ 0.34	$\downarrow$ 0.83	33.14 $\pm$ 0.16	32.82 $\pm$ 0.10	$\downarrow$ 0.97	32.64 $\pm$ 0.35	32.49 $\pm$ 0.38	$\downarrow$ 0.46	33.11 $\pm$ 0.22	32.80 $\pm$ 0.20	$\downarrow$ 0.94	32.62 $\pm$ 0.08	32.49 $\pm$ 0.08	$\downarrow$ 0.40	33.15 $\pm$ 0.27	32.73 $\pm$ 0.23	$\downarrow$ 1.27
	MAPE(%)	12.42 $\pm$ 0.01	12.37 $\pm$ 0.09	$\downarrow$ 0.40	14.74 $\pm$ 0.76	14.53 $\pm$ 0.41	$\downarrow$ 1.42	14.44 $\pm$ 0.47	14.43 $\pm$ 0.32	$\downarrow$ 0.07	14.15 $\pm$ 0.16	14.04 $\pm$ 0.15	$\downarrow$ 0.78	12.78 $\pm$ 0.17	12.72 $\pm$ 0.06	$\downarrow$ 0.47	13.72 $\pm$ 0.13	13.68 $\pm$ 0.24	$\downarrow$ 0.29
<i>PEMS-07</i>	MAE	21.67 $\pm$ 0.16	21.41 $\pm$ 0.13	$\downarrow$ 1.20	23.30 $\pm$ 0.81	23.08 $\pm$ 0.75	$\downarrow$ 0.94	22.62 $\pm$ 0.27	22.46 $\pm$ 0.27	$\downarrow$ 0.71	24.26 $\pm$ 0.23	23.83 $\pm$ 0.18	$\downarrow$ 1.77	21.72 $\pm$ 0.05	21.55 $\pm$ 0.05	$\downarrow$ 0.78	22.69 $\pm$ 0.15	22.50 $\pm$ 0.14	$\downarrow$ 0.84
	RMSE	37.48 $\pm$ 0.52	37.03 $\pm$ 0.48	$\downarrow$ 1.20	37.55 $\pm$ 0.91	37.24 $\pm$ 0.81	$\downarrow$ 0.83	36.87 $\pm$ 0.23	36.62 $\pm$ 0.26	$\downarrow$ 0.68	39.31 $\pm$ 0.26	38.63 $\pm$ 0.20	$\downarrow$ 1.73	36.24 $\pm$ 0.06	36.00 $\pm$ 0.06	$\downarrow$ 0.66	38.14 $\pm$ 0.44	37.77 $\pm$ 0.41	$\downarrow$ 0.97
	MAPE(%)	8.92 $\pm$ 0.05	8.87 $\pm$ 0.06	$\downarrow$ 0.56	10.08 $\pm$ 0.24	9.98 $\pm$ 0.24	$\downarrow$ 0.99	9.79 $\pm$ 0.16	9.75 $\pm$ 0.11	$\downarrow$ 0.41	10.57 $\pm$ 0.18	10.38 $\pm$ 0.07	$\downarrow$ 1.80	9.05 $\pm$ 0.03	9.00 $\pm$ 0.03	$\downarrow$ 0.55	9.94 $\pm$ 0.56	9.86 $\pm$ 0.33	$\downarrow$ 0.80
<i>PEMS-08</i>	MAE	14.84 $\pm$ 0.09	14.73 $\pm$ 0.08	$\downarrow$ 0.74	17.19 $\pm$ 0.17	17.07 $\pm$ 0.16	$\downarrow$ 0.70	16.37 $\pm$ 0.21	16.28 $\pm$ 0.20	$\downarrow$ 0.55	17.33 $\pm$ 0.19	17.17 $\pm$ 0.21	$\downarrow$ 0.92	15.61 $\pm$ 0.02	15.52 $\pm$ 0.02	$\downarrow$ 0.58	16.69 $\pm$ 0.06	16.56 $\pm$ 0.04	$\downarrow$ 0.78
	RMSE	25.61 $\pm$ 0.17	25.49 $\pm$ 0.16	$\downarrow$ 0.47	27.07 $\pm$ 0.30	26.93 $\pm$ 0.29	$\downarrow$ 0.52	26.14 $\pm$ 0.23	26.05 $\pm$ 0.21	$\downarrow$ 0.34	27.49 $\pm$ 0.21	27.31 $\pm$ 0.22	$\downarrow$ 0.65	25.70 $\pm$ 0.05	25.60 $\pm$ 0.05	$\downarrow$ 0.39	26.94 $\pm$ 0.10	26.80 $\pm$ 0.10	$\downarrow$ 0.52
	MAPE(%)	9.37 $\pm$ 0.04	9.32 $\pm$ 0.06	$\downarrow$ 0.53	11.27 $\pm$ 0.26	11.20 $\pm$ 0.28	$\downarrow$ 0.62	10.95 $\pm$ 0.34	10.79 $\pm$ 0.18	$\downarrow$ 1.46	11.63 $\pm$ 0.36	11.53 $\pm$ 0.30	$\downarrow$ 0.86	9.82 $\pm$ 0.12	9.76 $\pm$ 0.06	$\downarrow$ 0.61	11.46 $\pm$ 0.89	11.19 $\pm$ 0.38	$\downarrow$ 2.36
<i>KnowAir</i>	MAE	17.13 $\pm$ 0.19	17.06 $\pm$ 0.18	$\downarrow$ 0.41	17.14 $\pm$ 0.16	17.06 $\pm$ 0.16	$\downarrow$ 0.47	17.03 $\pm$ 0.07	16.94 $\pm$ 0.07	$\downarrow$ 0.53	17.03 $\pm$ 0.06	16.96 $\pm$ 0.06	$\downarrow$ 0.41	18.07 $\pm$ 0.11	17.98 $\pm$ 0.10	$\downarrow$ 0.50	17.07 $\pm$ 0.01	17.01 $\pm$ 0.02	$\downarrow$ 0.35
	RMSE	26.13 $\pm$ 0.20	26.06 $\pm$ 0.19	$\downarrow$ 0.27	26.18 $\pm$ 0.16	26.13 $\pm$ 0.16	$\downarrow$ 0.19	26.12 $\pm$ 0.15	26.05 $\pm$ 0.14	$\downarrow$ 0.27	26.14 $\pm$ 0.17	26.07 $\pm$ 0.17	$\downarrow$ 0.27	27.23 $\pm$ 0.02	27.17 $\pm$ 0.02	$\downarrow$ 0.22	26.45 $\pm$ 0.07	26.39 $\pm$ 0.06	$\downarrow$ 0.23
	MAPE(%)	62.14 $\pm$ 1.62	61.66 $\pm$ 1.53	$\downarrow$ 0.77	64.12 $\pm$ 1.24	63.15 $\pm$ 1.40	$\downarrow$ 1.51	64.51 $\pm$ 0.20	63.62 $\pm$ 0.28	$\downarrow$ 1.38	63.12 $\pm$ 0.97	62.70 $\pm$ 0.84	$\downarrow$ 0.67	70.00 $\pm$ 1.44	69.07 $\pm$ 1.35	$\downarrow$ 1.33	60.76 $\pm$ 0.34	60.50 $\pm$ 0.63	$\downarrow$ 0.43
<i>UrbanEV</i>	MAE	2.87 $\pm$ 0.02	2.85 $\pm$ 0.02	$\downarrow$ 0.70	3.04 $\pm$ 0.06	2.99 $\pm$ 0.06	$\downarrow$ 1.64	2.89 $\pm$ 0.03	2.85 $\pm$ 0.03	$\downarrow$ 1.38	3.29 $\pm$ 0.10	3.23 $\pm$ 0.10	$\downarrow$ 1.82	2.83 $\pm$ 0.01	2.79 $\pm$ 0.01	$\downarrow$ 1.41	3.09 $\pm$ 0.02	3.04 $\pm$ 0.02	$\downarrow$ 1.62
	RMSE	5.00 $\pm$ 0.01	4.98 $\pm$ 0.02	$\downarrow$ 0.40	5.09 $\pm$ 0.07	5.03 $\pm$ 0.07	$\downarrow$ 1.18	4.87 $\pm$ 0.07	4.81 $\pm$ 0.06	$\downarrow$ 1.23	5.63 $\pm$ 0.23	5.52 $\pm$ 0.22	$\downarrow$ 1.95	4.74 $\pm$ 0.02	4.67 $\pm$ 0.02	$\downarrow$ 1.48	5.31 $\pm$ 0.03	5.22 $\pm$ 0.02	$\downarrow$ 1.69
	MAPE(%)	27.14 $\pm$ 0.46	26.75 $\pm$ 0.58	$\downarrow$ 1.44	28.75 $\pm$ 0.08	28.22 $\pm$ 0.29	$\downarrow$ 1.84	29.10 $\pm$ 0.33	28.47 $\pm$ 0.26	$\downarrow$ 2.16	31.67 $\pm$ 0.97	31.45 $\pm$ 1.01	$\downarrow$ 0.70	27.60 $\pm$ 0.62	27.15 $\pm$ 0.43	$\downarrow$ 1.63	29.53 $\pm$ 0.57	29.26 $\pm$ 0.57	$\downarrow$ 0.91

**Competitive Effectiveness.** We further compare our method against various advanced approaches that can leverage test-time information. Since the official source code of *CompFormer* and *DOST* is not available and uses additional data information, it leads to an unfair comparison. Nevertheless, we still include all reported *METR-LA* benchmark values (indicated with  $*$ ) using a unified *GWNNet* backbone, categorized

into regular and online settings as presented in Table 3, based on their respective papers. Additionally, we implemented the popular *TTT-MAE* method as a surrogate for the unavailable *TTT-ST* method. Our observations are as follows: ❶ For the regular setting, our method achieves competitive results with more stable standard deviations. While other methods like *CompFormer* demonstrate similar performance, they often utilize more training information and computational resources. ❷ In the online setting, our method significantly outperforms existing approaches without requiring more complex model architecture modifications.

### 5.3 Universality Study (RQ2)

To demonstrate the universality of ST-TTC across diverse real-world scenarios, we explore various forecasting scenarios in the literature, including few-shot (Yuan et al., 2024c), long-term (Shao et al., 2022a), and large-scale (Han et al., 2024).

**Few-Shot Scenario.** To simulate limited training data, we retrained models using only the first 10% of existing training sets to investigate a more common and challenging few-shot scenario. Figure 2 shows the relative performance gains with ST-TTC (For full results, please refer Table E.1 in the Appendix). We observe: ❶ ST-TTC provides more significant improvements in the few-shot setting compared to the full-shot case in Table 2, with about half exceeding 2%. ❷ *KnowAir* shows the largest gain compared to other datasets, likely because its four-year long period leads to a substantial test distribution shift in the few-shot scenario, where our method adapts well.

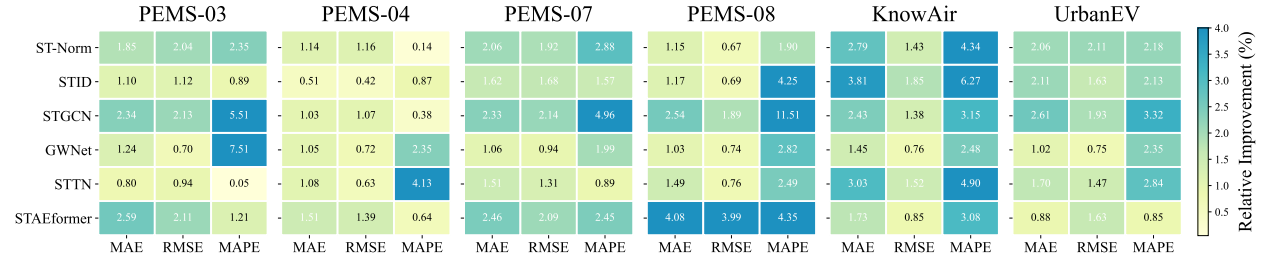


Figure 2 Relative improvements of different models w/ ST-TTC in the few-shot setting.

**Long-Term Scenario.** In real-world scenarios, long-term forecasting helps to further plan future decisions. We predicted 24 future steps from 24 past steps to explore more complex temporal changes. As shown in Figure 3, we present the relative performance improvement of the advanced *STID* model with our ST-TTC method, and give a test set prediction visualization case on the *PEMS-08* dataset (see Figure F.1 in the Appendix for more examples). Our observations include: ❶ ST-TTC consistently improves long-term forecasting, even more

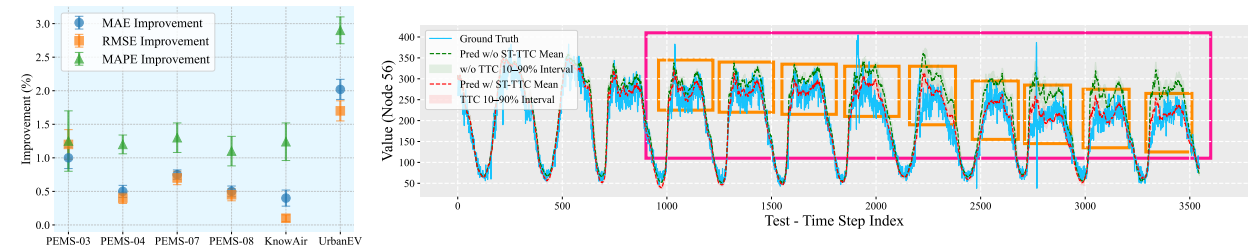


Figure 3 Left: relative improvement of long-term setting. Right: visualization study of *PEMS-08*.

Table 3 Performance comparison of the advanced method w/ ST-TTC on *METR-LA* benchmark. † means the results are statistically significant (t-test with p-value < 0.01).

Method	MAE	RMSE	w/o Training Set	w/o Modifying Backbone
<i>The training / validation / test set split used below is 70% / 10% / 20%.</i>				
<i>TTT-MAE</i> (Gandelsman et al., 2022)	3.47±0.03	7.43±0.05	✗	✓
<i>TENT</i> (Wang et al., 2021)	4.84±0.08	8.53±0.10	✓	✓
<i>CompFormer*</i> (Zhang et al., 2023c)	3.46±0.02	7.19±0.08	✗	✓
ST-TTC	3.46±0.01†	7.21±0.01	✓	✓
<i>The training / validation / test set split used below is 20% / 5% / 75%.</i>				
<i>OnlineTCN*</i> (Zinkevich, 2003)	4.78±0.03	8.70±0.04	✓	✗
<i>FSNet*</i> (Pham et al., 2023)	5.79±0.24	11.06±0.24	✓	✗
<i>OneNet*</i> (Wen et al., 2023)	4.94±0.03	8.80±0.06	✓	✗
<i>DOST*</i> (Wang et al., 2024c)	4.38±0.02	8.26±0.03	✓	✗
ST-TTC	3.77±0.07†	7.75±0.13†	✓	✓

than short-term (Table 2), likely due to more learnable information in longer windows. ② As the pink and orange box shows, our method learns test-time history, capturing both the global traffic decline and local fluctuations, leading to effective calibration.

**Large-Scale Scenario.** Beyond current regional datasets, state or national-level spatio-temporal forecasting can involve tens of thousands of stations and longer time frames. We explore large-scale scenarios using the popular *LargeST* benchmark (comprising *SD*, *GBA*, *GLA*, and *CA* subsets). Figure 4 illustrates the 12-step prediction performance gains of the state-of-the-art efficient spatio-temporal model *PatchSTG* (Fang et al., 2025) with our *ST-TTC*, along with a comparison of inference time complexity (For full results, see Table E.2 in Appendix). We observe: ① Our *ST-TTC* consistently yields further performance improvements across all datasets, even surpassing the improvement of the second-best baseline over the *PatchSTG* on some datasets. ② The additional inference time is at most 3.82 minutes, which is a clear advantage for the achieved performance gains compared to the training time cost of up to 14 hours.

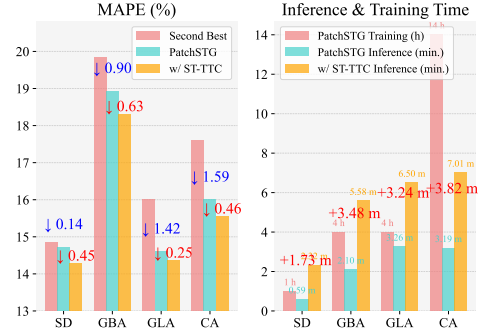


Figure 4 Performance on *LargeST*.

## 5.4 Flexibility Study (RQ3)

To illustrate the flexibility of *ST-TTC* in accommodating existing learning paradigms, we explore its integration with two training data-leveraging paradigms: OOD learning and Continual Learning.

**OOD Learning Setting.** Following prior work (Wang et al., 2024a), we use the *SD* dataset to simulate spatio-temporal shift. For the temporal dimension, we use 1-8/2019, 9-10/2019, and 11-12/2020 for training, validation, and testing, respectively. For the spatial dimension, we randomly mask 10% of nodes in the test set and consider three proportions of new nodes (10% / 15% / 20%) relative to the training node to mimic varying degrees of shift. In Figure 5, we present the 12-step average prediction performance gains of the advanced OOD learning model *STONE* with our *ST-TTC*, evaluated on all nodes and new nodes to demonstrate generalizability and scalability (Full results in Table E.3). We observe that: ① The *STONE* model with *ST-TTC* consistently achieves performance benefits, significantly outperforming all previous settings, indicating that existing OOD models are still insufficient for true OOD generalization, while our method is highly effective. ② For both all and new nodes, our improvements become more pronounced as the shift increases, further demonstrating our effectiveness in handling both generalizability and scalability in challenging scenarios.

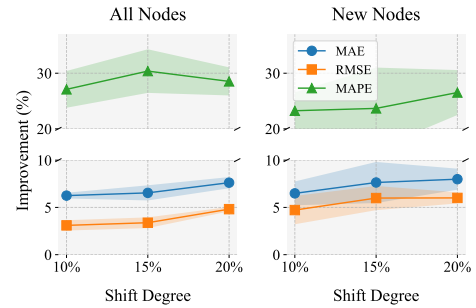


Figure 5 Relative improvement using our *ST-TTC* in the OOD learning setting.

**Continual Learning Setting.** Following prior work (Chen and Liang, 2025), we used multi-period streaming spatio-temporal data to examine our *ST-TTC*'s integration with continual learning method. Table 4 shows the improved 12-step forecasting of advanced continual learning models *EAC* and *STKEC* with our *ST-TTC*. We observed: ① Consistent performance gains for both models across all datasets; *STKEC* with *ST-TTC* even achieved comparable performance to best model *EAC*. ② *Energy-Stream* achieves significant improvement over other datasets, as the *ST-TTC* effectively learns and calibrates temporal changes, as shown by the frequency analysis (drastic shift changes) in Figure 6.

## 5.5 Mechanism & Robustness Study (RQ4)

We follow the OOD setup (challenging setting with 20% new nodes) to evaluate our *ST-TTC*.

**Strategy Study.** We compare different strategies: 1) simple nonlinear time domain calibration (*Time*), 2) learning only phase or amplitude modulation factors (*Pha.* / *Amp.*), 3) node-share modeling (*Node*), and

**Table 4** Performance comparison in continual learning setting.

Methods w/ ST-TTC	Air-Stream			PEMS-Stream			Energy-Stream			
	MAE	RMSE	MAPE(%)	MAE	RMSE	MAPE(%)	MAE	RMSE	MAPE(%)	
EAC	✗	24.15±0.14	38.22±0.31	31.79±0.05	14.92±0.11	24.17±0.17	20.82±0.16	5.15±0.10	5.46±0.09	50.55±2.60
	✓	23.54±0.15	37.51±0.27	31.44±0.10	14.71±0.07	23.87±0.12	20.53±0.03	3.47±0.01	3.94±0.00	39.66±0.41
	Δ	↓ 2.5%	↓ 1.9%	↓ 1.1%	↓ 1.4%	↓ 1.2%	↓ 1.4%	↓ 32.6%	↓ 27.8%	↓ 21.6%
STKEC	✗	25.44±1.05	40.11±1.13	33.30±1.64	16.25±0.04	26.73±0.07	22.33±0.16	5.41±0.15	5.72±0.10	52.40±1.10
	✓	24.26±0.05	39.02±0.05	31.73±0.04	16.05±0.06	26.39±0.11	21.88±0.06	3.83±0.09	4.28±0.08	43.22±0.90
	Δ	↓ 4.6%	↓ 2.7%	↓ 4.7%	↓ 1.2%	↓ 1.3%	↓ 2.0%	↓ 29.2%	↓ 25.2%	↓ 17.5%

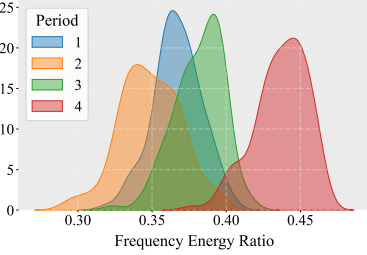
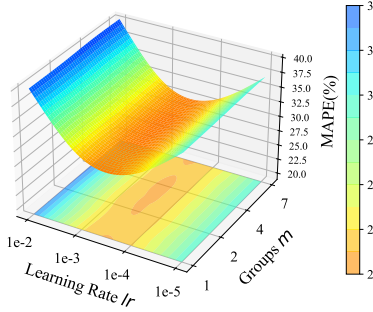
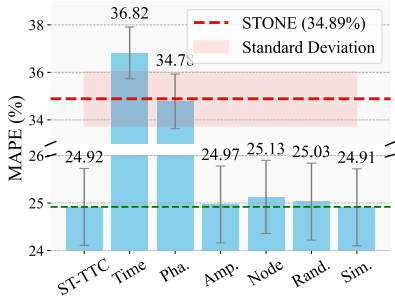


**Figure 6** Energy-Stream’s Shift.

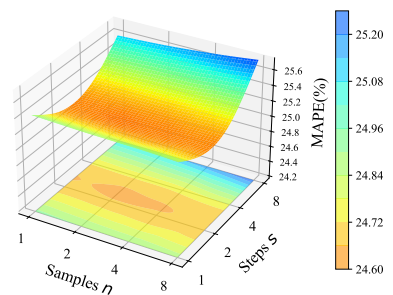


**Figure 7** Left: Strategy comparison. Middle: Effect of  $lr$  w.r.t  $m$ . Right: Effect of  $n$  w.r.t  $s$ .

4) random selection or retrieval of the most similar samples (*Rand.* / *Sim.*). As shown in Figure 7 left, we observe: ❶ Frequency-domain calibration significantly outperforms time-domain calibration, with amplitude modulation being the primary contributor; ❷ Sharing nodes leads to performance degradation due to spatial heterogeneity in spatio-temporal data; ❸ Random sample selection reduces performance, and retrieving similar samples offers negligible gains while incurring higher computational cost. Our proposed update strategy is already near-optimal.

**Parameter study.** We analyze the sensitivity of two parameter groups. As shown in the middle and right of Figure 7: ❶ Higher learning rates and fewer groups generally lead to poorer performance, likely due to limited parameter capacity hindering stable learning; ❷ Increasing the number of samples or update steps has minimal impact on performance (fluctuations < 1%), but significantly increases time cost, highlighting the rationale of our flash update mechanism.

### 5.6 Efficiency & Lightweight Study (RQ5)

**Result Analysis.** We use *GWNet* as the backbone and compare ST-TTC with other test-time adaptation methods on *METR-LA* in terms of total inference time and memory usage. As shown in Figure 8, ST-TTC achieves the best overall efficiency (excluding the *GWNet* baseline), being 4.64× faster and reducing memory usage by 37.12% compared to the least efficient method. These improvements are significant as they are much smaller than the sliding size (5 min.), thereby meeting the real-time requirements.

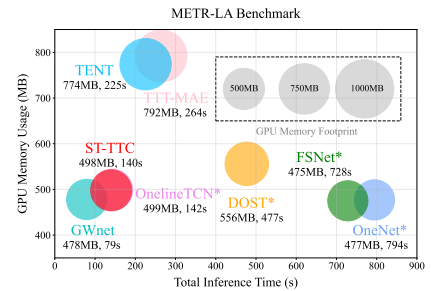


**Figure 8** time and memory.

## 6 Conclusion

In this paper, we investigate the objectives of test-time computation in spatio-temporal forecasting and explore effective approaches for its implementation. We propose ST-TTC, a novel paradigm that uses a flash gradient update with streaming memory queue to learning a spectral-domain calibrator via phase-amplitude modulation, effectively addressing non-stationary errors. Extensive experiments confirm its effectiveness, universality, and flexibility. In future work, we aim to explore how to enhance the internal computational capacity of spatio-temporal foundation models during test time.

## Acknowledgment

The first author would like to thank all the anonymous reviewers for their valuable comments and high recognition. Although he has almost lost his passion for this field and is ready to leave, he hopes that this study can still bring something new to the ST community.

This work is mainly supported by the National Natural Science Foundation of China (No. 62402414). This work is also supported by the Huawei Co., Ltd (No. TC20241023027), the Guangzhou-HKUST(GZ) Joint Funding Program (No. 2024A03J0620), Guangzhou Municipal Science and Technology Project (No. 2023A03J0011), the Guangzhou Industrial Information and Intelligent Key Laboratory Project (No. 2024A03J0628), and a grant from State Key Laboratory of Resources and Environmental Information System, and Guangdong Provincial Key Lab of Integrated Communication, Sensing and Computation for Ubiquitous Internet of Things (No. 2023B1212010007).

## References

- Ekin Akyürek, Mehul Damani, Adam Zweiger, Linlu Qiu, Han Guo, Jyothish Pari, Yoon Kim, and Jacob Andreas. The surprising effectiveness of test-time training for few-shot learning. [arXiv preprint arXiv:2411.07279](#), 2024.
- Mohammad Taha Bahadori, Qi Rose Yu, and Yan Liu. Fast multivariate spatio-temporal analysis via low rank tensor learning. [Advances in neural information processing systems](#), 27, 2014.
- Songran Bai, Yuheng Ji, Yue Liu, Xingwei Zhang, Xiaolong Zheng, and Daniel Dajun Zeng. Alleviating performance disparity in adversarial spatiotemporal graph learning under zero-inflated distribution. In [Proceedings of the AAAI Conference on Artificial Intelligence](#), volume 39, pages 11436–11444, 2025.
- Christoph Bergmeir. Fundamental limitations of foundational forecasting models: The need for multimodality and rigorous evaluation. In [Proc. NeurIPS Workshop](#), 2024.
- Bahar Biller and Barry L Nelson. Modeling and generating multivariate time-series input processes using a vector autoregressive technique. [ACM Transactions on Modeling and Computer Simulation \(TOMACS\)](#), 13(3):211–237, 2003.
- Léon Bottou and Vladimir Vapnik. Local learning algorithms. [Neural computation](#), 4(6):888–900, 1992.
- George EP Box and David A Pierce. Distribution of residual autocorrelations in autoregressive-integrated moving average time series models. [Journal of the American statistical Association](#), 65(332):1509–1526, 1970.
- Lorenzo Brigato, Rafael Morand, Knut Strømmen, Maria Panagiotou, Markus Schmidt, and Stavroula Mougiakakou. Position: There are no champions in long-term time series forecasting. [arXiv preprint arXiv:2502.14045](#), 2025.
- Changlu Chen, Yanbin Liu, Ling Chen, and Chengqi Zhang. Test-time training for spatial-temporal forecasting. In [Proceedings of the 2024 SIAM International Conference on Data Mining \(SDM\)](#), pages 463–471. SIAM, 2024.
- Wei Chen and Yuxuan Liang. Expand and compress: Exploring tuning principles for continual spatio-temporal graph forecasting. In [The Thirteenth International Conference on Learning Representations](#), 2025.
- Xu Chen, Junshan Wang, and Kunqing Xie. Trafficstream: A streaming traffic flow forecasting framework based on graph neural networks and continual learning. In [IJCAI](#), 2021.
- Andrea Cini, Ivan Marisca, Daniele Zambon, and Cesare Alippi. Taming local effects in graph-based spatiotemporal forecasting. [Advances in Neural Information Processing Systems](#), 36:55375–55393, 2023.
- AD Cliff and John K Ord. Space-time modelling with an application to regional forecasting. [Transactions of the Institute of British Geographers](#), pages 119–128, 1975.
- Noel Cressie and Christopher K Wikle. [Statistics for spatio-temporal data](#). John Wiley & Sons, 2011.
- Jinliang Deng, Xiusi Chen, Renhe Jiang, Xuan Song, and Ivor W Tsang. St-norm: Spatial and temporal normalization for multi-variate time series forecasting. In [Proceedings of the 27th ACM SIGKDD conference on knowledge discovery & data mining](#), pages 269–278, 2021.
- Jinliang Deng, Xiusi Chen, Renhe Jiang, Du Yin, Yi Yang, Xuan Song, and Ivor W Tsang. Disentangling structured components: Towards adaptive, interpretable and scalable time series forecasting. [IEEE Transactions on Knowledge and Data Engineering](#), 2024.

- Yuchen Fang, Yuxuan Liang, Bo Hui, Zezhi Shao, Liwei Deng, Xu Liu, Xinke Jiang, and Kai Zheng. Efficient large-scale traffic forecasting with transformers: A spatial data management perspective. In Proceedings of the 21th ACM SIGKDD international conference on knowledge discovery and data mining, 2025.
- Seth R Flaxman. Machine learning in space and time. PhD thesis, Ph. D. thesis, Carnegie Mellon University, 2015.
- A. Gammerman, V. Vovk, and V. Vapnik. Learning by transduction. In Proceedings of the Fourteenth Conference on Uncertainty in Artificial Intelligence, UAI'98, page 148–155, 1998.
- Yossi Gandelsman, Yu Sun, Xinlei Chen, and Alexei Efros. Test-time training with masked autoencoders. Advances in Neural Information Processing Systems, 35:29374–29385, 2022.
- Daya Guo, Dejian Yang, Haowei Zhang, Junxiao Song, Ruoyu Zhang, Runxin Xu, Qihao Zhu, Shirong Ma, Peiyi Wang, Xiao Bi, et al. Deepseek-r1: Incentivizing reasoning capability in llms via reinforcement learning. arXiv preprint arXiv:2501.12948, 2025.
- Pengxin Guo, Pengrong Jin, Ziyue Li, Lei Bai, and Yu Zhang. Online test-time adaptation of spatial-temporal traffic flow forecasting. arXiv preprint arXiv:2401.04148, 2024.
- Shengnan Guo, Youfang Lin, Ning Feng, Chao Song, and Huaiyu Wan. Attention based spatial-temporal graph convolutional networks for traffic flow forecasting. In Proceedings of the AAAI conference on artificial intelligence, volume 33, pages 922–929, 2019.
- Shengnan Guo, Youfang Lin, Huaiyu Wan, Xiucheng Li, and Gao Cong. Learning dynamics and heterogeneity of spatial-temporal graph data for traffic forecasting. IEEE Transactions on Knowledge and Data Engineering, 34(11): 5415–5428, 2021.
- Jindong Han, Weijia Zhang, Hao Liu, Tao Tao, Naiqiang Tan, and Hui Xiong. Bigst: Linear complexity spatio-temporal graph neural network for traffic forecasting on large-scale road networks. Proceedings of the VLDB Endowment, 17(5):1081–1090, 2024.
- Moritz Hardt and Yu Sun. Test-time training on nearest neighbors for large language models. In The Twelfth International Conference on Learning Representations, 2024.
- Peiyan Hu, Rui Wang, Xiang Zheng, Tao Zhang, Haodong Feng, Ruiqi Feng, Long Wei, Yue Wang, Zhi-Ming Ma, and Tailin Wu. Wavelet diffusion neural operator. 2025.
- Songtao Huang, Zhen Zhao, Can Li, and Lei Bai. Timekan: Kan-based frequency decomposition learning architecture for long-term time series forecasting. 2025.
- Aaron Jaech, Adam Kalai, Adam Lerer, Adam Richardson, Ahmed El-Kishky, Aiden Low, Alec Helyar, Aleksander Madry, Alex Beutel, Alex Carney, et al. Openai o1 system card. arXiv preprint arXiv:2412.16720, 2024.
- Minguk Jang, Sae-Young Chung, and Hye Won Chung. Test-time adaptation via self-training with nearest neighbor information. In The Eleventh International Conference on Learning Representations, 2023.
- Jiahao Ji, Wentao Zhang, Jingyuan Wang, and Chao Huang. Seeing the unseen: Learning basis confounder representations for robust traffic prediction. In Proceedings of the 31st ACM SIGKDD Conference on Knowledge Discovery and Data Mining V. 1, pages 577–588, 2025.
- Guangyin Jin, Yuxuan Liang, Yuchen Fang, Zezhi Shao, Jincai Huang, Junbo Zhang, and Yu Zheng. Spatio-temporal graph neural networks for predictive learning in urban computing: A survey. IEEE Transactions on Knowledge and Data Engineering, 36(10):5388–5408, 2023.
- Ming Jin, Huan Yee Koh, Qingsong Wen, Daniele Zambon, Cesare Alippi, Geoffrey I Webb, Irwin King, and Shirui Pan. A survey on graph neural networks for time series: Forecasting, classification, imputation, and anomaly detection. IEEE Transactions on Pattern Analysis and Machine Intelligence, 2024.
- Daniel Kahneman. Thinking, fast and slow. macmillan, 2011.
- Duc Kieu, Tung Kieu, Peng Han, Bin Yang, Christian S Jensen, and Bac Le. Team: Topological evolution-aware framework for traffic forecasting. Proceedings of the VLDB Endowment, 18(2):265–278, 2024.
- Rahul Kumar, Manish Bhanu, João Mendes-Moreira, and Joydeep Chandra. Spatio-temporal predictive modeling techniques for different domains: a survey. ACM Computing Surveys, 57(2):1–42, 2024.
- Ying-yee Ava Lau, Zhiwen Shao, and Dit-Yan Yeung. Fast and slow streams for online time series forecasting without information leakage. In The Thirteenth International Conference on Learning Representations, 2025.

- Sanghyun Lee and Chanyoung Park. Continual traffic forecasting via mixture of experts. [arXiv preprint arXiv:2406.03140](https://arxiv.org/abs/2406.03140), 2024.
- Han Li, Haohao Qu, Xiaojun Tan, Linlin You, Rui Zhu, and Wenqi Fan. Urbanev: An open benchmark dataset for urban electric vehicle charging demand prediction. [Scientific Data](https://www.sciencedirect.com/science/article/pii/S2405244632500000), page 523, 2025. ISSN 2052-4463. doi: 10.1038/s41597-025-04874-4.
- Yaguang Li, Rose Yu, Cyrus Shahabi, and Yan Liu. Diffusion convolutional recurrent neural network: Data-driven traffic forecasting. In [International Conference on Learning Representations](https://proceedings.mlr.press/v80/li18a.html), 2018.
- Zhonghang Li, Lianghao Xia, Jiabin Tang, Yong Xu, Lei Shi, Long Xia, Dawei Yin, and Chao Huang. Urbangpt: Spatio-temporal large language models. In [Proceedings of the 30th ACM SIGKDD Conference on Knowledge Discovery and Data Mining](https://proceedings.mlr.press/v162/li21a.html), pages 5351–5362, 2024a.
- Zhonghang Li, Lianghao Xia, Yong Xu, and Chao Huang. Flashst: A simple and universal prompt-tuning framework for traffic prediction. In [Proceedings of the 41st International Conference on Machine Learning](https://proceedings.mlr.press/v162/li21b.html), pages 28978–28988, 2024b.
- Zhonghang Li, Long Xia, Lei Shi, Yong Xu, Dawei Yin, and Chao Huang. Opencity: Open spatio-temporal foundation models for traffic prediction. [arXiv preprint arXiv:2408.10269](https://arxiv.org/abs/2408.10269), 2024c.
- Jian Liang, Dapeng Hu, and Jiashi Feng. Do we really need to access the source data? source hypothesis transfer for unsupervised domain adaptation. In [International conference on machine learning](https://proceedings.mlr.press/v139/liang20a.html), pages 6028–6039. PMLR, 2020.
- Jian Liang, Ran He, and Tieniu Tan. A comprehensive survey on test-time adaptation under distribution shifts. [International Journal of Computer Vision](https://www.sciencedirect.com/journal/international-journal-of-computer-vision), 133(1):31–64, 2025.
- Fan Liu, Hao Liu, and Wenzhao Jiang. Practical adversarial attacks on spatiotemporal traffic forecasting models. [Advances in Neural Information Processing Systems](https://www.sciencedirect.com/journal/advances-in-neural-information-processing-systems), 35:19035–19047, 2022.
- Hangchen Liu, Zheng Dong, Renhe Jiang, Jiewen Deng, Jinliang Deng, Qunjun Chen, and Xuan Song. Spatio-temporal adaptive embedding makes vanilla transformer sota for traffic forecasting. In [Proceedings of the 32nd ACM international conference on information and knowledge management](https://proceedings.mlr.press/v162/liu21a.html), pages 4125–4129, 2023a.
- Xu Liu, Yutong Xia, Yuxuan Liang, Junfeng Hu, Yiwei Wang, Lei Bai, Chao Huang, Zhenguang Liu, Bryan Hooi, and Roger Zimmermann. Largest: A benchmark dataset for large-scale traffic forecasting. In [Advances in Neural Information Processing Systems](https://proceedings.mlr.press/v162/liu21b.html), 2023b.
- Jiaming Ma, Pengkun Wang, Binwu Wang, Zhengyang Zhou, Xu Wang, Yudong Zhang, Du Qian, and Yang Wang. Stop! a out-of-distribution processor with robust spatiotemporal interaction. <https://openreview.net/forum?id=85WHuB5CUK>, 2024.
- Yurii Nesterov. [Introductory lectures on convex optimization: A basic course](https://www.springer.com/9781493998263), volume 87. Springer Science & Business Media, 2013.
- Tung Nguyen, Johannes Brandstetter, Ashish Kapoor, Jayesh K Gupta, and Aditya Grover. Climax: A foundation model for weather and climate. In [International Conference on Machine Learning](https://proceedings.mlr.press/v162/nguyen21a.html), pages 25904–25938. PMLR, 2023.
- Yuqi Nie, Nam H Nguyen, Phanwadee Sinthong, and Jayant Kalagnanam. A time series is worth 64 words: Long-term forecasting with transformers. In [The Eleventh International Conference on Learning Representations](https://proceedings.mlr.press/v162/nie21a.html), 2023.
- Orlando Ohashi and Luís Torgo. Wind speed forecasting using spatio-temporal indicators. In [ECAI 2012](https://www.springer.com/9781493998263), pages 975–980. IOS Press, 2012.
- Boris N Oreshkin, Arezou Amini, Lucy Coyle, and Mark Coates. Fc-gaga: Fully connected gated graph architecture for spatio-temporal traffic forecasting. In [Proceedings of the AAAI conference on artificial intelligence](https://proceedings.mlr.press/v139/oreshkin20a.html), volume 35, pages 9233–9241, 2021.
- Marc-Antoine Parseval. Mémoire sur les séries et sur l’intégration complète d’une équation aux différences partielles linéaires du second ordre, à coefficients constants. [Mém. prés. par divers savants, Acad. des Sciences, Paris](https://www.jstor.org/stable/2370311),(1), 1 (638-648):42, 1806.
- Phillip E Pfeifer and Stuart Jay Deutsch. A starima model-building procedure with application to description and regional forecasting. [Transactions of the Institute of British Geographers](https://www.jstor.org/stable/2610000), pages 330–349, 1980.
- Quang Pham, Chenghao Liu, Doyen Sahoo, and Steven Hoi. Learning fast and slow for online time series forecasting. In [The Eleventh International Conference on Learning Representations](https://proceedings.mlr.press/v162/pham21a.html), 2023.

- Ransalu Senanayake, Simon O’callaghan, and Fabio Ramos. Predicting spatio-temporal propagation of seasonal influenza using variational gaussian process regression. In Proceedings of the AAAI conference on artificial intelligence, volume 30, 2016.
- Wei Shao, Zhiling Jin, Shuo Wang, Yufan Kang, Xiao Xiao, Hamid Menouar, Zhaofeng Zhang, Junshan Zhang, and Flora Salim. Long-term spatio-temporal forecasting via dynamic multiple-graph attention. In 31st International Joint Conference on Artificial Intelligence, IJCAI 2022, pages 2225–2232. International Joint Conferences on Artificial Intelligence, 2022a.
- Wei Shao, Yufan Kang, Ziyang Peng, Xiao Xiao, Lei Wang, Yuhui Yang, and Flora D Salim. Stemo: Early spatio-temporal forecasting with multi-objective reinforcement learning. In Proceedings of the 30th ACM SIGKDD Conference on Knowledge Discovery and Data Mining, pages 2618–2627, 2024a.
- ZeZhi Shao, Zhao Zhang, Fei Wang, Wei Wei, and Yongjun Xu. Spatial-temporal identity: A simple yet effective baseline for multivariate time series forecasting. In Proceedings of the 31st ACM international conference on information & knowledge management, pages 4454–4458, 2022b.
- ZeZhi Shao, Fei Wang, Yongjun Xu, Wei Wei, Chengqing Yu, Zhao Zhang, Di Yao, Tao Sun, Guangyin Jin, Xin Cao, et al. Exploring progress in multivariate time series forecasting: Comprehensive benchmarking and heterogeneity analysis. IEEE Transactions on Knowledge and Data Engineering, 2024b.
- Xingjian Shi and Dit-Yan Yeung. Machine learning for spatiotemporal sequence forecasting: A survey. arXiv preprint arXiv:1808.06865, 2018.
- Charlie Victor Snell, Jaehoon Lee, Kelvin Xu, and Aviral Kumar. Scaling llm test-time compute optimally can be more effective than scaling parameters for reasoning. In The Thirteenth International Conference on Learning Representations, volume 2, page 7, 2025.
- Chao Song, Youfang Lin, Shengnan Guo, and Huaiyu Wan. Spatial-temporal synchronous graph convolutional networks: A new framework for spatial-temporal network data forecasting. In Proceedings of the AAAI conference on artificial intelligence, volume 34, pages 914–921, 2020.
- Yu Sun, Xiaolong Wang, Zhuang Liu, John Miller, Alexei Efros, and Moritz Hardt. Test-time training with self-supervision for generalization under distribution shifts. In International conference on machine learning, pages 9229–9248. PMLR, 2020.
- Vladimir Vapnik. The nature of statistical learning theory. Springer science & business media, 1999.
- Binwu Wang, Yudong Zhang, Jiahao Shi, Pengkun Wang, Xu Wang, Lei Bai, and Yang Wang. Knowledge expansion and consolidation for continual traffic prediction with expanding graphs. IEEE Transactions on Intelligent Transportation Systems, 24(7):7190–7201, 2023a.
- Binwu Wang, Yudong Zhang, Xu Wang, Pengkun Wang, Zhengyang Zhou, Lei Bai, and Yang Wang. Pattern expansion and consolidation on evolving graphs for continual traffic prediction. In Proceedings of the 29th ACM SIGKDD Conference on Knowledge Discovery and Data Mining, pages 2223–2232, 2023b.
- Binwu Wang, Jiaming Ma, Pengkun Wang, Xu Wang, Yudong Zhang, Zhengyang Zhou, and Yang Wang. Stone: A spatio-temporal ood learning framework kills both spatial and temporal shifts. In Proceedings of the 30th ACM SIGKDD Conference on Knowledge Discovery and Data Mining, pages 2948–2959, 2024a.
- Binwu Wang, Pengkun Wang, Yudong Zhang, Xu Wang, Zhengyang Zhou, Lei Bai, and Yang Wang. Towards dynamic spatial-temporal graph learning: A decoupled perspective. In Proceedings of the AAAI Conference on Artificial Intelligence, volume 38, pages 9089–9097, 2024b.
- Chengxin Wang, Gary Tan, Swagato Barman Roy, and Beng Chin Ooi. Distribution-aware online continual learning for urban spatio-temporal forecasting. arXiv preprint arXiv:2411.15893, 2024c.
- Dequan Wang, Evan Shelhamer, Shaoteng Liu, Bruno Olshausen, and Trevor Darrell. Tent: Fully test-time adaptation by entropy minimization. In The Ninth International Conference on Learning Representations, 2021.
- Hongjun Wang, Jiyuan Chen, Tong Pan, Zheng Dong, Lingyu Zhang, Renhe Jiang, and Xuan Song. Evaluating the generalization ability of spatiotemporal model in urban scenario. arXiv preprint arXiv:2410.04740, 2024d.
- Hongjun Wang, Jiyuan Chen, Tong Pan, Zheng Dong, Lingyu Zhang, Renhe Jiang, and Xuan Song. Robust traffic forecasting against spatial shift over years. arXiv preprint arXiv:2410.00373, 2024e.
- Huaizhi Wang, Zhenxing Lei, Xian Zhang, Bin Zhou, and Jianchun Peng. A review of deep learning for renewable energy forecasting. Energy Conversion and Management, 198:111799, 2019.

- Qin Wang, Olga Fink, Luc Van Gool, and Dengxin Dai. Continual test-time domain adaptation. In Proceedings of the IEEE/CVF Conference on Computer Vision and Pattern Recognition, pages 7201–7211, 2022.
- Renhao Wang, Yu Sun, Arnub Tandon, Yossi Gandelsman, Xinlei Chen, Alexei A Efros, and Xiaolong Wang. Test-time training on video streams. Journal of Machine Learning Research, 26(9):1–29, 2025a.
- Shuo Wang, Yanran Li, Jiang Zhang, Qingye Meng, Lingwei Meng, and Fei Gao. Pm2. 5-gnn: A domain knowledge enhanced graph neural network for pm2. 5 forecasting. In Proceedings of the 28th international conference on advances in geographic information systems, pages 163–166, 2020.
- Yuxuan Wang, Haixu Wu, Yuezhou Ma, Yuchen Fang, Ziyi Zhang, Yong Liu, Shiyu Wang, Zhou Ye, Yang Xiang, Jianmin Wang, et al. Accuracy law for the future of deep time series forecasting. arXiv preprint arXiv:2510.02729, 2025b.
- Qingsong Wen, Weiqi Chen, Liang Sun, Zhang Zhang, Liang Wang, Rong Jin, Tieniu Tan, et al. Onenet: Enhancing time series forecasting models under concept drift by online ensembling. Advances in Neural Information Processing Systems, 36:69949–69980, 2023.
- Hao Wu, Fan Xu, Chong Chen, Xian-Sheng Hua, Xiao Luo, and Haixin Wang. Pastnet: Introducing physical inductive biases for spatio-temporal video prediction. In Proceedings of the 32nd ACM International Conference on Multimedia, pages 2917–2926, 2024.
- Zonghan Wu, Shirui Pan, Guodong Long, Jing Jiang, and Chengqi Zhang. Graph wavenet for deep spatial-temporal graph modeling. arXiv preprint arXiv:1906.00121, 2019.
- Yutong Xia, Yuxuan Liang, Haomin Wen, Xu Liu, Kun Wang, Zhengyang Zhou, and Roger Zimmermann. Deciphering spatio-temporal graph forecasting: A causal lens and treatment. Advances in Neural Information Processing Systems, 36:37068–37088, 2023.
- Chen Xu, Qiang Wang, Wenqi Zhang, and Chen Sun. Spatiotemporal ego-graph domain adaptation for traffic prediction with data missing. IEEE Transactions on Intelligent Transportation Systems, 2024a.
- Mingxing Xu, Wenrui Dai, Chunmiao Liu, Xing Gao, Weiyao Lin, Guo-Jun Qi, and Hongkai Xiong. Spatial-temporal transformer networks for traffic flow forecasting. arXiv preprint arXiv:2001.02908, 2020.
- Zhijian Xu, Ailing Zeng, and Qiang Xu. Fits: Modeling time series with  $10k$  parameters. In The Twelfth International Conference on Learning Representations, 2024b.
- Kun Yi, Qi Zhang, Wei Fan, Hui He, Liang Hu, Pengyang Wang, Ning An, Longbing Cao, and Zhendong Niu. Fouriernn: Rethinking multivariate time series forecasting from a pure graph perspective. Advances in neural information processing systems, 36:69638–69660, 2023.
- Zhongchao Yi, Zhengyang Zhou, Qihe Huang, Yanjiang Chen, Liheng Yu, Xu Wang, and Yang Wang. Get rid of isolation: A continuous multi-task spatio-temporal learning framework. In The Thirty-eighth Annual Conference on Neural Information Processing Systems, 2024.
- Bing Yu, Haoteng Yin, and Zhanxing Zhu. Spatio-temporal graph convolutional networks: a deep learning framework for traffic forecasting. In Proceedings of the 27th International Joint Conference on Artificial Intelligence, pages 3634–3640, 2018.
- Xie Yu, Jingyuan Wang, Yifan Yang, Qian Huang, and Ke Qu. Bigcity: A universal spatiotemporal model for unified trajectory and traffic state data analysis. arXiv preprint arXiv:2412.00953, 2024.
- Yuan Yuan, Jingtao Ding, Jie Feng, Depeng Jin, and Yong Li. Unist: A prompt-empowered universal model for urban spatio-temporal prediction. In Proceedings of the 30th ACM SIGKDD Conference on Knowledge Discovery and Data Mining, pages 4095–4106, 2024a.
- Yuan Yuan, Chonghua Han, Jingtao Ding, Depeng Jin, and Yong Li. Urbandit: A foundation model for open-world urban spatio-temporal learning. arXiv preprint arXiv:2411.12164, 2024b.
- Yuan Yuan, Chenyang Shao, Jingtao Ding, Depeng Jin, and Yong Li. Spatio-temporal few-shot learning via diffusive neural network generation. In The Twelfth International Conference on Learning Representations, 2024c.
- Yang Yue, Zhiqi Chen, Rui Lu, Andrew Zhao, Zhaokai Wang, Shiji Song, and Gao Huang. Does reinforcement learning really incentivize reasoning capacity in llms beyond the base model? arXiv preprint arXiv:2504.13837, 2025.
- Ailing Zeng, Muxi Chen, Lei Zhang, and Qiang Xu. Are transformers effective for time series forecasting? In Proceedings of the AAAI conference on artificial intelligence, volume 37, pages 11121–11128, 2023.

- Qianru Zhang, Chao Huang, Lianghao Xia, Zheng Wang, Zhonghang Li, and Siuming Yiu. Automated spatio-temporal graph contrastive learning. In Proceedings of the ACM Web Conference 2023, pages 295–305, 2023a.
- Qianru Zhang, Chao Huang, Lianghao Xia, Zheng Wang, Siu Ming Yiu, and Ruihua Han. Spatial-temporal graph learning with adversarial contrastive adaptation. In International Conference on Machine Learning, pages 41151–41163. PMLR, 2023b.
- Qiyuan Zhang, Fuyuan Lyu, Zexu Sun, Lei Wang, Weixu Zhang, Zhihan Guo, Yufei Wang, Irwin King, Xue Liu, and Chen Ma. What, how, where, and how well? a survey on test-time scaling in large language models. arXiv preprint arXiv:2503.24235, 2025.
- Zhiwei Zhang, Weizhong Zhang, Yaowei Huang, and Kani Chen. Test-time compensated representation learning for extreme traffic forecasting. arXiv preprint arXiv:2309.09074, 2023c.
- Vincent Zhihao Zheng, Seongjin Choi, and Lijun Sun. Probabilistic traffic forecasting with dynamic regression. Transportation Science, 2025.
- Yu Zheng, Xiuwen Yi, Ming Li, Ruiyuan Li, Zhangqing Shan, Eric Chang, and Tianrui Li. Forecasting fine-grained air quality based on big data. In Proceedings of the 21th ACM SIGKDD international conference on knowledge discovery and data mining, pages 2267–2276, 2015.
- Zhengyang Zhou, Qihe Huang, Kuo Yang, Kun Wang, Xu Wang, Yudong Zhang, Yuxuan Liang, and Yang Wang. Maintaining the status quo: Capturing invariant relations for ood spatiotemporal learning. In Proceedings of the 29th ACM SIGKDD conference on knowledge discovery and data mining, pages 3603–3614, 2023.
- Zhengyang Zhou, Qihe Huang, Binwu Wang, Jianpeng Hou, Kuo Yang, Yuxuan Liang, and Yang Wang. Coms2t: A complementary spatiotemporal learning system for data-adaptive model evolution. arXiv preprint arXiv:2403.01738, 2024.
- Martin Zinkevich. Online convex programming and generalized infinitesimal gradient ascent. In Proceedings of the 20th international conference on machine learning (icml-03), pages 928–936, 2003.

# Appendix

---

## Table of Contents

<b>A More Related Work</b>	<b>17</b>
A.1 Spectral Domain Learning. . . . .	17
A.2 Online Learning for Forecasting. . . . .	18
A.3 Test-Time Adaptation. . . . .	18
<b>B Theoretical Analysis</b>	<b>18</b>
B.1 Approximate Bound on Output Perturbation . . . . .	18
B.2 Controlled Descent on Streaming Memory Queues . . . . .	19
<b>C Method Details</b>	<b>20</b>
C.1 Spectral Domain Calibrator . . . . .	20
C.2 Lightning Gradient Update . . . . .	21
<b>D Experimental Details</b>	<b>23</b>
D.1 Datasets Details . . . . .	23
D.2 Baseline Details . . . . .	24
D.3 Protocol Details . . . . .	26
<b>E More Results</b>	<b>27</b>
E.1 Complete Results Table . . . . .	27
E.2 Visualization Case . . . . .	27
<b>F More Discussion</b>	<b>28</b>
F.1 Distinction between Spatio-Temporal Forecasting and Long-Term Time Series . . . . .	28
F.2 Limitation . . . . .	29
F.3 Future Work . . . . .	30
<b>G Broader Impacts</b>	<b>30</b>

---

## A More Related Work

### A.1 Spectral Domain Learning.

Many recent forecasting models leverage spectral (Fourier or wavelet) representations to capture periodic or multiscale patterns in spatio-temporal data. For example, *PastNet* (Wu et al., 2024) integrates a Fourier-domain convolutional operator to embed physical inductive biases, achieving state-of-the-art results in weather and traffic prediction. *FourierGNN* (Yi et al., 2023) builds a learnable Fourier-graph operator that conducts

graph convolutions in the frequency domain, reducing convolutional complexity from  $\mathcal{O}(n^2)$  to  $\mathcal{O}(n)$ . Wavelet-based methods like *WDNO* (Hu et al., 2025) perform diffusion modeling in the wavelet domain to capture abrupt spatio-temporal changes and multi-resolution features. In the pure time-series setting, approaches such as *FITS* (Xu et al., 2024b) interpolate in the complex Fourier domain and discard negligible high-frequency components to maintain accuracy with very few parameters, and *TimeKAN* (Huang et al., 2025) explicitly decomposes multivariate series into multiple frequency bands using Kolmogorov–Arnold networks. These works demonstrate how frequency-domain learning can improve forecasting efficiency and accuracy by isolating dominant spectral components. *Different from these methods, our method combines spectral domain feature extraction with calibration-aware test-time computation to achieve reliable and calibrated forecasts even under changing conditions.*

## A.2 Online Learning for Forecasting.

Traditional online forecasting methods include adaptive filters like Kalman filters and recursive least squares that update linear models on streaming data. Recently, deep-learning approaches have been proposed to handle nonstationarity in an online fashion. For instance, *FSNet* (Pham et al., 2023) implements a complementary “fast and slow” learning system: a fast-adapting component for sudden pattern changes and a slow memory component for repeating trends. *OneNet* (Wen et al., 2023) runs two parallel neural forecasters (one modeling temporal dependencies, one modeling cross-variable dependencies) and uses reinforcement learning to dynamically weight their predictions under concept drift. These methods continuously update model parameters or ensemble weights as new data arrive. A recent study (Lau et al., 2025) pointed out the information leakage problem of previous online time series prediction methods, where the model makes predictions and then evaluates them based on the historical time steps that have been back-propagated for parameter updates. By redefining the setting to focus on predicting unknown future steps and evaluating unobserved data points, they propose a two-stream framework for online prediction, DSOE, which is conceptually similar to previous methods, generating predictions in a coarse-to-fine manner through a teacher-student model. *Compared with these methods, we focus on the more difficult spatio-temporal predictions while not requiring complex network architecture design. Instead, we propose a calibration-aware framework that focuses on adjusting predictions online instead of learning predictions.*

## A.3 Test-Time Adaptation.

Recent test-time adaptation techniques can be grouped by their adaptation strategy. *Entropy minimization* methods adjust a trained model to increase prediction confidence on unlabeled test data. For example, (Wang et al., 2021) propose *TENT*, which adapts model parameters by minimizing the entropy of its predictions on each test batch and updating batch-normalization layers online. *Feature alignment* methods recalibrate feature distributions using test inputs; for instance, adaptive batch-normalization techniques re-estimate BN statistics on the target data to align feature distributions without labels. *Self-supervised adaptation* uses auxiliary tasks on the test data to refine the model. Test-Time Training (Gandelsman et al., 2022; Hardt and Sun, 2024; Sun et al., 2020; Wang et al., 2025a) converts each test input into a self-supervised learning problem (e.g. predicting image rotations) and updates model parameters before making a prediction. Similarly, SHOT (Liang et al., 2020) freezes the source classifier and updates the feature extractor on unlabeled target data using pseudo-labeling and information maximization. Each of these paradigms improves generalization under distribution shift without access to target labels. *In contrast, unlike these methods that exploit self-supervisory information, our spatio-temporal prediction setting can use labels from historical test information, enabling explicit optimization of the objective at test time, ensuring real-time adaptivity.*

# B Theoretical Analysis

## B.1 Approximate Bound on Output Perturbation

**Theorem 1** (Approximate Bound on Output Perturbation). *Let  $Y \in \mathbb{C}^{B \times N \times M}$  be the original frequency-domain representation of the backbone’s prediction  $y \in \mathbb{R}^{B \times N \times T}$ , and  $y' \in \mathbb{R}^{B \times N \times T}$  be the calibrated output. Suppose the amplitude and phase modulation parameters satisfy  $|\lambda_g^\alpha| \leq \epsilon_\alpha$  and  $|\lambda_g^\phi| \leq \epsilon_\phi$  for all groups*

$g \in \{1, \dots, G\}$ . Then, the  $\ell_2$ -norm of the calibration error satisfies:

$$\|y' - y\|_2 \leq (\epsilon_\alpha + \epsilon_\phi) \|Y\|_2,$$

where  $\|Y\|_2$  is the  $\ell_2$ -norm of  $Y$ .

*Proof.* Let  $\Delta Y = Y' - Y$  denote the frequency-domain perturbation. For each group  $g$ , the calibrated spectrum is  $Y'_g = A_g(1 + \lambda_g^\alpha)e^{j(P_g + \lambda_g^\phi)}$ . Expanding  $Y'_g$  around  $\lambda_g^\alpha = 0, \lambda_g^\phi = 0$ , we approximate:

$$Y'_g \approx Y_g(1 + \lambda_g^\alpha + j\lambda_g^\phi),$$

where higher-order terms (e.g.,  $\lambda_g^\alpha \lambda_g^\phi$ ) are neglected under small  $\epsilon_\alpha, \epsilon_\phi$ . Thus, the perturbation is:

$$\Delta Y_g \approx Y_g(\lambda_g^\alpha + j\lambda_g^\phi).$$

The  $\ell_2$ -norm of  $\Delta Y$  is bounded by:

$$\|\Delta Y\|_2^2 = \sum_{g=1}^G \sum_{f \in \text{Group } g} |\Delta Y_{g,f}|^2 \leq \sum_{g=1}^G (\epsilon_\alpha^2 + \epsilon_\phi^2) \sum_{f \in \text{Group } g} |Y_{g,f}|^2 = (\epsilon_\alpha^2 + \epsilon_\phi^2) \|Y\|_2^2.$$

By Parseval's theorem (Parseval, 1806),  $\|y' - y\|_2 = \|\Delta Y\|_2$ , hence:

$$\|y' - y\|_2 \leq \sqrt{\epsilon_\alpha^2 + \epsilon_\phi^2} \|Y\|_2 \leq (\epsilon_\alpha + \epsilon_\phi) \|Y\|_2.$$

□

**Remark 1.** This theorem guarantees that the calibration-induced perturbation is sub-linearly bounded by the modulation parameters  $\epsilon_\alpha, \epsilon_\phi$ . By constraining these parameters (e.g., via regularization during test-time adaptation), SD-Calibrator ensures the calibrated output does not deviate excessively from the original prediction, thereby avoiding overfitting to transient noise. The group-wise parameterization further reduces the effective degrees of freedom (from  $\mathcal{O}(NM)$  to  $\mathcal{O}(NG)$ ), inherently limiting the risk of over-parameterization.

## B.2 Controlled Descent on Streaming Memory Queues

**Assumption 1** (Lipschitz Continuous Gradient of the Loss). The loss function  $L_k(\lambda) = \mathcal{L}(g_\lambda(f_\theta(X_o^{(k)})), Y_o^{(k)})$  is differentiable with respect to  $\lambda$ , and its gradient  $\nabla_\lambda L_k(\lambda)$  is Lipschitz continuous with constant  $L_c > 0$ . That is, for any  $\lambda_a, \lambda_b$ :

$$\|\nabla_\lambda L_k(\lambda_a) - \nabla_\lambda L_k(\lambda_b)\|_2 \leq L_c \|\lambda_a - \lambda_b\|_2$$

According to the descent Lemma (Nesterov, 2013), this implies:

$$L_k(\lambda_b) \leq L_k(\lambda_a) + \langle \nabla_\lambda L_k(\lambda_a), \lambda_b - \lambda_a \rangle + \frac{L_c}{2} \|\lambda_b - \lambda_a\|_2^2$$

**Assumption 2** (Bounded Gradient). The norm of the gradient of the loss function with respect to the calibrator parameters  $\lambda$  is bounded for any sample  $(X_o^{(k)}, Y_o^{(k)})$  from the queue and any reasonable parameter set  $\lambda_k$ :

$$\|\nabla_\lambda L_k(\lambda_k)\|_2 \leq G_{max}$$

for some constant  $G_{max} > 0$ .

This is a common assumption, especially if the output of the calibrator and the true labels are within a certain range, and the calibrator  $g_\lambda$  is well-behaved.

**Proposition 2** (Controlled Descent on Streaming Memory Queues). *Let the above assumptions hold. For the  $k$ -th update step using the dequeued sample pair  $(X_o^{(k)}, Y_o^{(k)})$ , if the learning rate  $\eta$  satisfies  $0 < \eta < \frac{2}{L_c}$ , then the single gradient descent step on the SD-Calibrator parameters  $\lambda$  ensures a decrease in the loss function for that specific sample:*

$$L_k(\lambda_{k+1}) \leq L_k(\lambda_k) - \eta \left(1 - \frac{L_c \eta}{2}\right) \|\nabla_\lambda L_k(\lambda_k)\|_2^2$$

Furthermore, the change in the calibrator parameters is bounded:

$$\|\lambda_{k+1} - \lambda_k\|_2 \leq \eta G_{max}$$

*Proof.* Let  $L_k(\lambda) = \mathcal{L}(g_\lambda(f_\theta(X_o^{(k)})), Y_o^{(k)})$  be the loss for the  $k$ -th dequeued sample. The parameter update rule is  $\lambda_{k+1} = \lambda_k - \eta \nabla_\lambda L_k(\lambda_k)$ .

From Assumption 1, we have:

$$L_k(\lambda_{k+1}) \leq L_k(\lambda_k) + \langle \nabla_\lambda L_k(\lambda_k), \lambda_{k+1} - \lambda_k \rangle + \frac{L_c}{2} \|\lambda_{k+1} - \lambda_k\|_2^2$$

Substitute  $\lambda_{k+1} - \lambda_k = -\eta \nabla_\lambda L_k(\lambda_k)$ :

$$L_k(\lambda_{k+1}) \leq L_k(\lambda_k) + \langle \nabla_\lambda L_k(\lambda_k), -\eta \nabla_\lambda L_k(\lambda_k) \rangle + \frac{L_c}{2} \|\eta \nabla_\lambda L_k(\lambda_k)\|_2^2$$

$$L_k(\lambda_{k+1}) \leq L_k(\lambda_k) - \eta \|\nabla_\lambda L_k(\lambda_k)\|_2^2 + \frac{L_c \eta^2}{2} \|\nabla_\lambda L_k(\lambda_k)\|_2^2$$

Factor out  $\|\nabla_\lambda L_k(\lambda_k)\|_2^2$ :

$$L_k(\lambda_{k+1}) \leq L_k(\lambda_k) - \eta \left(1 - \frac{L_c \eta}{2}\right) \|\nabla_\lambda L_k(\lambda_k)\|_2^2$$

For the loss to decrease (or stay the same if gradient is zero), we require the term  $\eta \left(1 - \frac{L_c \eta}{2}\right) \|\nabla_\lambda L_k(\lambda_k)\|_2^2 \geq 0$ .

Since  $\eta > 0$  and  $\|\nabla_\lambda L_k(\lambda_k)\|_2^2 \geq 0$ , we need  $\left(1 - \frac{L_c \eta}{2}\right) > 0$ . This implies  $1 > \frac{L_c \eta}{2}$ , so  $\frac{2}{L_c} > \eta$ . Thus, if  $0 < \eta < \frac{2}{L_c}$ , the loss  $L_k(\lambda_{k+1})$  on the sample  $(X_o^{(k)}, Y_o^{(k)})$  is strictly reduced if  $\nabla_\lambda L_k(\lambda_k) \neq 0$ .

For the bound on parameter change:

$$\|\lambda_{k+1} - \lambda_k\|_2 = \|\eta \nabla_\lambda L_k(\lambda_k)\|_2 = \eta \|\nabla_\lambda L_k(\lambda_k)\|_2$$

Using Assumption 2,  $\|\nabla_\lambda L_k(\lambda_k)\|_2 \leq G_{max}$ :

$$\|\lambda_{k+1} - \lambda_k\|_2 \leq \eta G_{max}$$

This completes the proof.  $\square$

**Remark 2.** *The proposition demonstrates that each single-step update is not arbitrary but moves the SD-Calibrator's parameters  $\lambda$  in a direction that reduces the prediction error on the specific historical sample  $(X_o^{(k)}, Y_o^{(k)})$  used for the update, provided the learning rate  $\eta$  is chosen appropriately (i.e., small enough, specifically  $\eta < 2/L_c$ ). The condition on  $\eta$  ensures that the update step does not overshoot. The second part,  $\|\lambda_{k+1} - \lambda_k\|_2 \leq \eta G_{max}$ , shows that the magnitude of change in the parameters  $\lambda$  during each update is bounded. This is crucial for preventing the calibrator from experiencing excessively large or erratic parameter shifts from one step to the next, which could lead to instability or overfitting to noisy individual samples.*

## C Method Details

### C.1 Spectral Domain Calibrator

**Algorithm Workflow.** We summarize the algorithm workflow of Section 4.1 in Algorithm 1.

**Algorithm Pseudo-code.** We further present Algorithm 1 in the form of pytorch pseudo code in Listing 1 for easy understanding.

## C.2 Lightning Gradient Update

**Algorithm Pseudo-code.** We summarize the algorithm workflow of Section 4.2 in Algorithm 2.

**Algorithm Workflow.** We further present Algorithm 2 in the form of pytorch pseudo code in Listing 2 for easy understanding.

---

### Algorithm 1 Spectral Domain Calibrator

---

**Require:** Pre-trained backbone  $f_\theta$ , Test input  $x$ , Horizon length  $T$ , Number of nodes  $N$ , Groups  $G$

**Ensure:** Calibrated output  $\hat{y}^{\text{cal}}$

- 1: Get the backbone predictions:  $\hat{y} = f_\theta(x) \in \mathbb{R}^{N \times T}$
  - 2: Compute  $M \leftarrow \frac{T}{2} + 1$ 
    - ▷ **I: Spatial-aware Decomposition**
  - 3: Apply real-to-complex FFT along time dimension for each node:  $Y_f \leftarrow \text{rFFT}(\hat{y}) \in \mathbb{C}^{N \times M}$
  - 4: Decompose:  $A \leftarrow |Y_f|$ ,  $P \leftarrow \angle Y_f$ 
    - ▷ **II: Group-wise Modulation**
  - 5: **for**  $g = 1, \dots, G$  **do**
    - 6: Get group index:  $start \leftarrow (g - 1)\lfloor M/G \rfloor + 1$ ,  $end \leftarrow \begin{cases} M & g = G \\ g\lfloor M/G \rfloor & \text{otherwise} \end{cases}$
    - 7: Get learnable offsets:  $\lambda_g^\alpha \in \mathbb{R}^{N \times 1}$ ,  $\lambda_g^\phi \in \mathbb{R}^{N \times 1}$
    - 8: Modulate group-slice:  $A'_g \leftarrow A[:, start : end] \odot (1 + \lambda_g^\alpha)$ ,  $P'_g \leftarrow P[:, start : end] + \lambda_g^\phi$
    - 9: Reconstruct slice:  $Y'_f[:, start : end] \leftarrow A'_g \odot e^{jP'_g}$
  - 10: **end for**
    - ▷ **III: Inverse Transform**
  - 11: Inverse FFT:  $\hat{y}^{\text{cal}} \leftarrow \text{irFFT}(Y'_f) \in \mathbb{R}^{N \times T}$
  - 12: **return**  $\hat{y}^{\text{cal}}$
- 

### Listing 1 PyTorch-style pseudocode: SD-Calibrator Class

```
class SD_Calibrator(nn.Module):
    """
    Spectral Domain Calibrator with Phase-Amplitude Modulation
    """

    def __init__(self, num_nodes, freq_bins, groups=4):
        """
        Args:
            num_nodes: number of spatial nodes (N)
            freq_bins: number of frequency bins (M = T // 2 + 1)
            groups: number of frequency groups (G)
        """
        super().__init__()
        self.groups = groups
        self.group_size = freq_bins // groups

        # Learnable offsets for amplitude and phase: (G, N, 1)
        self.lambda_amp = nn.Parameter(
            torch.zeros(groups, num_nodes, 1)
        )
        self.lambda_phi = nn.Parameter(
            torch.zeros(groups, num_nodes, 1)
        )

    def forward(self, y_pred):
        """
```

```

Args:
    y_pred: prediction from backbone, shape (B, 1, N, T)
           B defaults to 1, because only one sample can be tested
Returns:
    calibrated prediction, shape (B, 1, N, T)
"""
B, _, N, T = y_pred.shape
y = y_pred[:, 0] # (B, N, T)

Yf = torch.fft.rfft(y, dim=-1) # (B, N, M)
A = torch.abs(Yf)
P = torch.angle(Yf)

Yf_corr = torch.zeros_like(Yf)
for g in range(self.groups):
    start = g * self.group_size
    if g == self.groups - 1:
        end = T // 2 + 1
    else:
        end = (g + 1) * self.group_size

    lam_a = self.lambda_amp[g].unsqueeze(0) # (1, N, 1)
    lam_p = self.lambda_phi[g].unsqueeze(0)

    A_g = A[:, :, start:end] * (1 + lam_a)
    P_g = P[:, :, start:end] + lam_p

    Yf_corr[:, :, start:end] = A_g * torch.exp(1j * P_g)

y_time = torch.fft.irfft(Yf_corr, n=T, dim=-1)
return y_time.unsqueeze(1) # (B, 1, N, T)

```

---

### Algorithm 2 Flash Gradient Update Mechanism

---

**Require:** Test spatio-temporal sample stream  $\{x_t\}_{t=1}^B$ , Pre-trained backbone  $f_\theta$ , Streaming memory queue  $\mathcal{Q}$ , Queue size  $T$  (equal to horizon length)

**Ensure:** Spectral domain calibrator  $g_\theta$ , Prediction collection of test samples  $\{\hat{y}_t^{cal}\}_{t=1}^B$

- 1: Initialize Calibrator module  $g_\theta = (\lambda^\alpha, \lambda^\phi)$ , empty queue  $\mathcal{Q}$
  - 2: **for** each timestep  $t = 1, 2, \dots$  **do**
  - 3:   Receive  $x_t$ , compute default prediction  $\hat{y}_t = f_\theta(x_t)$ 
    - ▷ **I: Streaming Memory Queue**
  - 4:   Use Algorithm 1 to obtain the calibration results:  $\hat{y}_t^{cal} = g_\theta(\hat{y}_t; \lambda)$
  - 5:   Record ground truth:  $y_t$  (collected by the value of  $x_t$ , available  $T$  time steps in the future)
  - 6:    $\mathcal{Q}$ .enqueue( $(x_t, y_t)$ )
    - ▷ **II: Flash Gradient Update**
  - 7:   **if**  $\text{len}(\mathcal{Q}) > T$  **then**
  - 8:      $(x_o, y_o) = \mathcal{Q}$ .dequeue()
  - 9:     Use Algorithm 1 to obtain the calibration results:  $\hat{y}_o^{cal} = f_\theta(x_o)$
  - 10:    Update:  $\lambda \leftarrow \lambda - \eta \nabla_\lambda L(y_o, \hat{y}_o^{cal})$
  - 11:   **end if**
  - 12: **end for**
  - 13: **return**  $g_\theta, \{\hat{y}_t^{cal}\}_{t=1}^B$
- 

### Listing 2 PyTorch-style pseudocode: Flash Gradient Update Function

---

```

def st_ttc_test(self, test_loader, node_num, T, groups):
    """
    Flash Gradient Update with Streaming Memory Queue
    """
    SDC = SD_Calibrator(node_num, T//2+1, groups).to(self.device)
    optimizer = torch.optim.Adam(SDC.parameters(), lr=1e-4)
    loss_fn = self._select_criterion()
    SMQ, preds = Queue(maxsize=T), []

    for x, y in test_loader:
        x, y = x.to(self.device), y.to(self.device)
        with torch.no_grad():
            y_pred = self.model(x)
            y_corr = SDC(y_pred)

        # Use y_corr for inference
        y_corr = self.scaler.inverse_transform(y_corr)
        preds.append(y_corr.cpu().detach().numpy())

    SMQ.put((x, y))
    if SMQ.full():
        x_old, y_old = SMQ.get()
        with torch.no_grad():
            y_pred_old = self.model(x_old)

        SDC.train()
        y_corr_old = SDC(y_pred_old)
        y_corr_old = self.scaler.inverse_transform(y_corr_old)

        loss = loss_fn(y_corr_old, y_old)
        loss.backward()
        optimizer.step()
        optimizer.zero_grad()
        SDC.eval()

    return preds

```

## D Experimental Details

### D.1 Datasets Details

Our experiments are carried out on 14 real-world datasets from different domains. The statistics of these spatio-temporal datasets are shown in Table D.1.

We follow the conventional practice (Li et al., 2018) to define the graph topology for all spatio-temporal datasets except Know-Air. Specifically, we construct the adjacency matrix  $A$  for each dataset using a threshold Gaussian kernel, defined as follows:

$$A_{[ij]} = \begin{cases} \exp\left(-\frac{d_{ij}^2}{\sigma^2}\right) & \text{if } \exp\left(-\frac{d_{ij}^2}{\sigma^2}\right) \geq r \text{ and } i \neq j \\ 0 & \text{otherwise} \end{cases}$$

where  $d_{ij}$  represents the distance between sensors  $i$  and  $j$ ,  $\sigma$  is the standard deviation of all distances, and  $r$  is the threshold. We follow the recommended parameter settings in all corresponding papers.

For the KnowAir dataset, we follow the original paper (Wang et al., 2020) and calculate the correlation between nodes to construct the adjacency matrix. Intuitively, most aerosol pollutants are distributed within a

certain range above the ground. In addition, the mountains along the two cities will hinder the transmission of pollutants to the  $\text{PM}_{2.5}$  direction. Based on these intuitions, we constrain the weights in the adjacency matrix by the following formula:

$$A_{[ij]} = H(d_\theta - d_{ij}) \cdot H(m_\theta - m_{ij}), \quad \text{where}$$

$$d_{ij} = \|\rho_i - \rho_j\|, \quad m_{ij} = \sup_{\lambda \in (0,1)} \{h(\lambda\rho_i + (1-\lambda)\rho_j) - \max\{h(\rho_i), h(\rho_j)\}\},$$

where  $\rho_i$  is the location (latitude, longitude) of node  $i$ ,  $h(\rho)$  is the height of location  $\rho$ , and  $\|\cdot\|$  is the L2-norm of the vector.  $H(\cdot)$  is the Heaviside step function, where  $H(x) = 1$  if and only if  $x > 0$ .  $d_\theta$  and  $m_\theta$  are the distance and altitude thresholds, respectively. Specifically, we also set the distance threshold  $d_\theta = 300$  km and the altitude threshold  $m_\theta = 1200$  meters.

**Table D.1** Summary of datasets used for our experiments. Degree: the average degree of each node. Meta: the number of metadata associated with each node. Data Points: multiplication of nodes and frames. M: million ( $10^6$ ).

Source	Dataset	Nodes	Time Range	Frames	Sampling Rate	Data Points
(Song et al., 2020)	PEMS03	358	09/01/2018 – 11/30/2018	26,208	5 minutes	9.38M
	PEMS04	307	01/01/2018 – 02/28/2018	16,992	5 minutes	5.22M
	PEMS07	883	05/01/2017 – 08/06/2017	28,224	5 minutes	24.92M
	PEMS08	170	07/01/2016 – 08/31/2016	17,856	5 minutes	3.04M
(Li et al., 2025)	UrbanEV	275	09/01/2022 – 02/28/2023	4344	1 hour	1.19M
(Wang et al., 2020)	Know-Air	184	01/01/2015 – 12/31/2018	11688	3 hours	2.15M
(Li et al., 2018)	METR-LA	207	03/01/2012 – 06/27/2012	34,272	5 minutes	7.09M
LargeST (Liu et al., 2023b)	CA	8,600	01/01/2019 – 12/31/2019	35,040	15 minutes	30.13M
	GLA	3,834	01/01/2019 – 12/31/2019	35,040	15 minutes	13.43M
	GBA	2,352	01/01/2019 – 12/31/2019	35,040	15 minutes	8.87M
	SD	716	01/01/2019 – 12/31/2020	70,080	15 minutes	5.02M
(Chen and Liang, 2025)	Air-Stream	1087 → 1154 → 1193 → 1202	01/01/2016 - 12/31/2019	34065	1 hour	15.79M
	PEMS-Stream	655 → 715 → 786 → 822 → 834 → 850 → 871	07/10/2011 - 09/08/2017	61,992	5 minutes	34.30M
	Energy-Stream	103 → 113 → 122 → 134	Unknown (245 days)	34,560	10 minutes	1.63M

## D.2 Baseline Details

In our paper, we cover various spatio-temporal forecasting methods under various learning paradigms. The following is a classification and brief introduction of these advanced methods:

### Classical Learning Methods for Spatio-Temporal Forecasting.

- *STAEformer* (Liu et al., 2023a): *STAEformer* is a spatial-temporal adaptive embedding transformer that makes vanilla transformer state-of-the-art for spatio-temporal forecasting. It introduces a novel architecture to effectively capture the dynamic spatial and temporal dependencies in spatio-temporal data. <https://github.com/XDZhelheim/STAEformer>
- *STTN* (Xu et al., 2020): *STTN* is a spatial-temporal transformer network designed for traffic flow forecasting. It leverages dynamic directed spatial dependencies and long-range temporal dependencies to enhance the accuracy of long-term traffic predictions. <https://github.com/xumingxingsjtu/STTN>
- *GWNet* (Wu et al., 2019): *GWNet* is a graph wavenet model for deep spatial-temporal graph modeling. It effectively captures the complex spatial and temporal patterns in spatio-temporal data using a combination

of graph convolutional networks and dilated causal convolutions. <https://github.com/nanzhan/Graph-WaveNet>

- *STGCN* (Yu et al., 2018): *STGCN* is a spatio-temporal graph convolutional network framework for traffic forecasting. It integrates graph convolutional networks with temporal convolutional networks to model the spatial and temporal dependencies in traffic data. <https://github.com/hazdzz/stgcn>
- *STID* (Shao et al., 2022b): *STID* is a simple yet effective baseline for spatio-temporal forecasting. It addresses the indistinguishability of samples in spatial and temporal dimensions by attaching spatial and temporal identity information, achieving competitive performance with concise and efficient models. <https://github.com/GestaltCogTeam/STID>
- *ST-Norm* (Deng et al., 2021): *ST-Norm* is a method that applies spatial and temporal normalization for multi-variate time series forecasting. It enhances the performance of forecasting models by normalizing the spatial and temporal features of the data. <https://github.com/JLDeng/ST-Norm>

### Efficient Learning Methods for Large-Scale Spatio-Temporal Forecasting.

- *PatchSTG* (Fang et al., 2025): *PatchSTG* is an attention-based dynamic spatial modeling method that uses irregular spatial patching for efficient large-scale spatio-temporal forecasting. It reduces computational complexity by segmenting large-scale inputs into balanced and non-overlapped patches, capturing local and global spatial dependencies effectively. <https://github.com/lmissher/patchstg>

### OOD Learning Methods for Spatio-Temporal Forecasting.

- *STONE* (Wang et al., 2024a): *STONE* is a state-of-the-art spatio-temporal OOD learning framework that effectively models spatial heterogeneity and generates temporal and spatial semantic graphs. It introduces a graph perturbation mechanism to enhance the model’s environmental modeling capability for better generalization. <https://github.com/PoorOtterBob/STONE-KDD-2024>

### Continual Learning Methods for Spatio-Temporal Forecasting.

- *EAC* (Chen and Liang, 2025): *EAC* is a state-of-the-art method for exploring the rapid adaptation of models in the face of dynamic spatio-temporal graph changes during supervised finetuning. It follows the principles of expand and compress to address the challenges of retraining models over new data and catastrophic forgetting. <https://github.com/Onedean/EAC>
- *STKEC* (Wang et al., 2023a): *STKEC* is a continual learning framework for traffic flow prediction on expanding traffic networks. It introduces a pattern bank to store representative network patterns and employs a pattern expansion mechanism to incorporate new patterns from evolving networks without requiring historical graph data. <https://github.com/wangbinwu13116175205/STKEC>

In addition to these advanced spatio-temporal forecasting models, we also cover various competitive baselines that learn with test information, mainly in the following three categories:

### Popular test-time training methods

- *TTT-MAE* (Gandelsman et al., 2022): *TTT-MAE* is a test-time training method that uses masked autoencoders to adjust the model during inference. It helps improve the performance of the model on unseen data by effectively utilizing test-time information. We adapt it to the backbone model of the spatiotemporal network, which is divided into a feature extractor and a prediction head as well as a self-supervisory head. <https://github.com/Rima-ag/TTT-MAE>
- *TENT* (Wang et al., 2021): *TENT* is a method for adjusting the model at test time by normalizing the activation function to reduce the offset between the training distribution and the test distribution. It enhances the generalization ability of the model without retraining on labeled test data. Although it is theoretically designed mainly for the cross entropy loss function, that is, classification tasks, we can still directly apply it to our prediction scenarios. <https://github.com/DequanWang/tent>

### Classical online time series forecasting methods

- *OnlineTCN* (Zinkevich, 2003): *OnlineTCN* is an online learning method based on a time convolutional

network. It can adapt to new data sequentially and is very suitable for real-time prediction applications where data arrives continuously. <https://github.com/locuslab/TCN>

- *FSNet* (Pham et al., 2023): *FSNet* proposes a fast and slow learning network for online time series prediction that can handle both sudden changes and repeated patterns. In particular, *FSNet* improves on a slowly learning backbone by dynamically balancing fast adaptation to recent changes and retrieval of similar old knowledge. *FSNet* implements this mechanism through the interaction between two complementary components of the adapter to monitor each layer’s contribution to missing events, and an associative memory that supports remembering, updating, and recalling repeated events. <https://github.com/salesforce/fsnet>
- *OneNet* (Wen et al., 2023): *OneNet* dynamically updates and combines two models, one focusing on modeling dependencies across time dimensions and the other focusing on cross-variable dependencies. The approach integrates reinforcement learning-based methods into a traditional online convex programming framework, allowing the two models to be linearly combined with dynamically adjusted weights, thereby addressing the main drawback of classical online prediction methods that are slow to adapt to concept drift. <https://github.com/yfzhang114/OneNet>

### Advanced spatio-temporal forecasting methods using test information.

- *CompFormer* (Zhang et al., 2023c): *CompFormer* proposes a test-time compensated representation learning framework, including a spatiotemporal decomposed database and a multi-head spatial transformer model. The former component explicitly separates all training data along the time dimension according to periodic features, while the latter component establishes connections between recent observations and historical sequences in the database through a spatial attention matrix. This enables it to transfer robust features to overcome abnormal events
- *DOST* (Wang et al., 2024c): *DOST* proposes a novel online continuous learning framework tailored to the characteristics of spatiotemporal data. *DOST* adopts an adaptive spatiotemporal network equipped with variable independent adapters to dynamically address the unique distribution changes of each urban location. In addition, to adapt to the gradual nature of these transformations, a wake-sleep learning strategy is used, which intermittently fine-tunes the adapters during the online stage to reduce computational overhead.

## D.3 Protocol Details

**Metrics Detail.** We use different metrics such as MAE, RMSE, and MAPE. Formally, these metrics are formulated as following:

$$\text{MAE} = \frac{1}{n} \sum_{i=1}^n |y_i - \hat{y}_i|, \quad \text{RMSE} = \sqrt{\frac{1}{n} \sum_{i=1}^n (y_i - \hat{y}_i)^2}, \quad \text{MAPE} = \frac{100\%}{n} \sum_{i=1}^n \left| \frac{\hat{y}_i - y_i}{y_i} \right|$$

where  $n$  represents the indices of all observed samples,  $y_i$  denotes the  $i$ -th actual sample, and  $\hat{y}_i$  is the corresponding prediction.

**Parameter Detail.** For the hyper-parameter settings of all baseline methods, we follow the parameter settings recommended by the corresponding references. For our paper, except for the robustness study section, all other experimental hyper-parameters are set uniformly: the learning rate  $lr$  is  $1e-4$ , and the number of groups  $m$  is set to 4. All experiments are conducted on a Linux server equipped with a  $1 \times$  AMD EPYC 7763 128-Core Processor CPU (256GB memory) and  $4 \times$  NVIDIA RTX A6000 (48GB memory) GPUs. To carry out benchmark testing experiments, all baselines are set to run for a duration of 100~150 epochs by default (depends on the corresponding paper), with specific timings contingent upon the method with early stop mechanism. The number of early stopping steps is set to 10.

## E More Results

### E.1 Complete Results Table

We provide complete information of the experimental tables in the main text as Table E.1, E.2, E.3

**Table E.1** Performance comparison of different models w/ and w/o ST-TTC in the few-shot scenario.

Models		Transformer-based				Graph-based				MLP-based			
		<i>STAEformer</i> (Liu et al., 2023a)		<i>STTN</i> (Xu et al., 2020)		<i>GWNet</i> (Wu et al., 2019)		<i>STGCN</i> (Yu et al., 2018)		<i>STID</i> (Shao et al., 2022b)		<i>ST-Norm</i> (Deng et al., 2021)	
w/ ST-TTC		✗	✓	✗	✓	✗	✓	✗	✓	✗	✓	✗	✓
<i>PEMS-03</i>	MAE	23.57±0.90	<b>22.96</b> ±0.93	21.32±0.93	<b>21.15</b> ±0.92	21.70±0.98	<b>21.43</b> ±0.92	21.79±0.50	<b>21.28</b> ±0.54	21.81±0.24	<b>21.57</b> ±0.24	21.13±0.31	<b>20.74</b> ±0.28
	RMSE	37.90±1.41	<b>37.10</b> ±1.59	34.19±1.59	<b>33.87</b> ±1.53	34.52±1.44	<b>34.28</b> ±1.40	34.82±0.92	<b>34.08</b> ±0.89	35.58±0.53	<b>35.18</b> ±0.52	33.76±0.45	<b>33.07</b> ±0.35
	MAPE(%)	21.49±1.21	<b>21.23</b> ±1.03	21.14±1.35	<b>21.13</b> ±1.28	21.30±1.14	<b>19.70</b> ±0.57	<b>22.85</b> ±0.76	<b>21.59</b> ±0.77	21.46±0.86	<b>21.27</b> ±0.73	<b>22.57</b> ±3.13	<b>22.04</b> ±2.22
<i>PEMS-04</i>	MAE	35.10±4.25	<b>34.57</b> ±4.08	29.76±0.37	<b>29.44</b> ±0.31	33.22±1.86	<b>32.87</b> ±1.95	29.97±0.81	<b>29.66</b> ±0.83	29.64±0.67	<b>29.49</b> ±0.65	30.66±0.11	<b>30.31</b> ±0.14
	RMSE	50.94±4.86	<b>50.23</b> ±4.59	44.17±0.75	<b>43.89</b> ±0.81	50.09±2.56	<b>49.73</b> ±2.73	45.96±1.26	<b>45.47</b> ±1.28	44.81±1.13	<b>44.62</b> ±1.10	45.86±0.50	<b>45.33</b> ±0.49
	MAPE(%)	23.55±3.28	<b>23.40</b> ±3.26	23.51±1.27	<b>22.54</b> ±0.71	22.97±3.52	<b>22.43</b> ±3.17	20.80±1.19	<b>20.72</b> ±1.19	22.90±1.77	<b>22.70</b> ±1.72	21.75±0.67	<b>21.72</b> ±0.60
<i>PEMS-07</i>	MAE	30.45±0.47	<b>29.70</b> ±0.39	31.70±0.82	<b>31.22</b> ±0.69	33.17±0.65	<b>32.82</b> ±0.63	32.64±0.72	<b>31.88</b> ±0.77	31.42±1.00	<b>30.91</b> ±1.05	31.14±0.06	<b>30.50</b> ±0.05
	RMSE	47.89±0.81	<b>46.89</b> ±0.76	46.57±1.10	<b>45.96</b> ±0.93	49.83±0.59	<b>49.36</b> ±0.57	48.65±0.14	<b>47.61</b> ±0.05	47.51±0.82	<b>46.71</b> ±0.97	47.45±0.43	<b>46.54</b> ±0.42
	MAPE(%)	13.87±0.27	<b>13.53</b> ±0.23	14.58±0.02	<b>14.45</b> ±0.13	15.04±0.70	<b>14.74</b> ±0.58	17.13±1.40	<b>16.28</b> ±0.99	15.27±1.15	<b>15.03</b> ±1.20	14.60±0.67	<b>14.18</b> ±0.46
<i>PEMS-08</i>	MAE	36.98±7.31	<b>35.47</b> ±6.03	24.17±0.42	<b>23.81</b> ±0.41	26.21±0.85	<b>25.94</b> ±0.97	25.97±0.25	<b>25.31</b> ±0.21	24.03±0.27	<b>23.75</b> ±0.28	24.34±0.09	<b>24.06</b> ±0.07
	RMSE	54.61±10.46	<b>52.43</b> ±8.37	36.89±0.45	<b>36.61</b> ±0.50	40.81±0.95	<b>40.51</b> ±1.11	38.53±0.15	<b>37.80</b> ±0.10	37.62±0.77	<b>37.36</b> ±0.77	37.45±0.16	<b>37.20</b> ±0.20
	MAPE(%)	27.38±9.55	<b>26.19</b> ±8.29	18.10±0.52	<b>17.65</b> ±0.54	17.00±1.10	<b>16.52</b> ±1.25	20.16±1.91	<b>17.84</b> ±0.88	15.07±0.53	<b>14.43</b> ±0.20	15.28±0.59	<b>14.99</b> ±0.29
<i>KnowAir</i>	MAE	18.48±0.50	<b>18.16</b> ±0.35	20.47±0.23	<b>19.85</b> ±0.23	19.32±0.32	<b>19.04</b> ±0.29	20.59±0.26	<b>20.09</b> ±0.25	22.58±1.20	<b>21.72</b> ±0.94	21.52±0.39	<b>20.92</b> ±0.36
	RMSE	27.20±0.09	<b>26.97</b> ±0.08	28.95±0.44	<b>28.51</b> ±0.46	27.79±0.13	<b>27.58</b> ±0.15	29.05±0.20	<b>28.65</b> ±0.21	30.25±1.03	<b>29.69</b> ±0.83	29.28±0.44	<b>28.86</b> ±0.41
	MAPE(%)	72.37±7.17	<b>70.14</b> ±4.89	85.39±1.82	<b>81.21</b> ±1.63	80.49±5.43	<b>78.49</b> ±5.40	84.80±2.40	<b>82.13</b> ±2.18	102.09±6.60	<b>95.69</b> ±5.08	95.24±2.26	<b>91.11</b> ±1.80
<i>UrbanEV</i>	MAE	3.39±0.12	<b>3.36</b> ±0.07	4.12±0.06	<b>4.05</b> ±0.06	3.92±0.09	<b>3.88</b> ±0.09	4.21±0.10	<b>4.10</b> ±0.10	3.31±0.06	<b>3.24</b> ±0.05	4.85±0.10	<b>4.75</b> ±0.11
	RMSE	6.15±0.21	<b>6.05</b> ±0.16	6.81±0.06	<b>6.71</b> ±0.05	6.64±0.12	<b>6.59</b> ±0.11	6.74±0.19	<b>6.61</b> ±0.17	5.51±0.10	<b>5.42</b> ±0.08	8.54±0.27	<b>8.36</b> ±0.27
	MAPE(%)	31.60±0.19	<b>31.33</b> ±0.47	38.41±1.43	<b>37.32</b> ±1.33	35.79±1.24	<b>34.95</b> ±1.10	40.93±1.48	<b>39.57</b> ±1.52	31.42±0.59	<b>30.75</b> ±0.50	43.20±1.28	<b>42.26</b> ±1.25

**Table E.2** PatchSTG with ST-TTC in LargeST Benchmark.

Datasets	Methods	Horizon 3			Horizon 6			Horizon 12			Average		
		MAE	RMSE	MAPE(%)	MAE	RMSE	MAPE(%)	MAE	RMSE	MAPE(%)	MAE	RMSE	MAPE(%)
<i>SD</i>	PatchSTG	14.53	24.34	9.22	16.86	28.63	11.11	20.66	36.27	14.72	16.90	29.27	11.23
	w/ ST-TTC	14.44	24.07	8.70	16.66	28.18	10.93	20.37	35.68	14.27	16.72	28.83	11.11
	Δ	↓ 0.6%	↓ 1.1%	↓ 5.6%	↓ 1.2%	↓ 1.6%	↓ 1.6%	↓ 1.4%	↓ 1.6%	↓ 3.1%	↓ 1.1%	↓ 1.5%	↓ 1.1%
<i>GBA</i>	PatchSTG	16.81	28.71	12.25	19.68	33.09	14.51	23.49	39.23	18.93	19.50	33.16	14.64
	w/ ST-TTC	16.65	28.31	12.12	19.30	32.40	14.35	22.96	38.33	18.30	19.16	32.49	14.48
	Δ	↓ 1.0%	↓ 1.4%	↓ 1.1%	↓ 1.9%	↓ 2.1%	↓ 1.1%	↓ 2.3%	↓ 2.3%	↓ 3.3%	↓ 1.7%	↓ 2.0%	↓ 1.1%
<i>GLA</i>	PatchSTG	15.84	26.34	9.27	19.06	31.85	11.30	23.32	39.64	14.60	18.96	32.33	11.44
	w/ ST-TTC	15.78	26.08	9.15	18.76	31.29	11.21	22.86	38.89	14.35	18.69	31.78	11.36
	Δ	↓ 0.4%	↓ 1.0%	↓ 1.3%	↓ 1.6%	↓ 1.8%	↓ 0.8%	↓ 2.0%	↓ 1.9%	↓ 1.7%	↓ 1.4%	↓ 1.7%	↓ 0.7%
<i>CA</i>	PatchSTG	14.69	24.82	10.51	17.41	29.43	12.83	21.20	36.13	16.00	17.35	29.79	12.79
	w/ ST-TTC	14.59	24.61	10.40	17.14	28.97	12.51	20.76	35.38	15.54	17.10	29.31	12.53
	Δ	↓ 0.7%	↓ 0.8%	↓ 1.0%	↓ 1.6%	↓ 1.6%	↓ 2.5%	↓ 2.1%	↓ 2.1%	↓ 2.9%	↓ 1.4%	↓ 1.6%	↓ 2.0%

### E.2 Visualization Case

We provide more visualization examples of test set predictions to illustrate the effectiveness of our calibration, as shown in Figure F.1

**Table E.3** Performance of spatio-temporal shift dataset SD-ratio(%) on all nodes and unknown new nodes at different spatio-temporal shift levels.

Dataset	Horizon	Methods	All Node			New Node		
			MAE	RMSE	MAPE(%)	MAE	RMSE	MAPE(%)
SD-10%	12	STONE	40.74 $\pm$ 4.24	58.43 $\pm$ 3.67	45.82 $\pm$ 9.30	46.25 $\pm$ 7.02	66.97 $\pm$ 7.05	47.57 $\pm$ 8.02
		w/ ST-TTC	39.41 $\pm$ 3.82	57.44 $\pm$ 3.67	38.02 $\pm$ 5.19	44.65 $\pm$ 6.69	65.06 $\pm$ 6.95	41.85 $\pm$ 5.87
		$\Delta$	$\downarrow$ 3.3%	$\downarrow$ 1.7%	$\downarrow$ 17.0%	$\downarrow$ 3.5%	$\downarrow$ 2.9%	$\downarrow$ 12.0%
	Avg.	STONE	30.18 $\pm$ 1.19	42.83 $\pm$ 1.38	39.44 $\pm$ 3.03	32.79 $\pm$ 2.77	46.68 $\pm$ 3.87	40.12 $\pm$ 0.30
		w/ ST-TTC	28.29 $\pm$ 1.04	41.50 $\pm$ 1.16	28.66 $\pm$ 1.32	30.66 $\pm$ 2.63	44.44 $\pm$ 3.32	30.80 $\pm$ 1.54
		$\Delta$	$\downarrow$ 6.3%	$\downarrow$ 3.1%	$\downarrow$ 27.3%	$\downarrow$ 6.5%	$\downarrow$ 4.8%	$\downarrow$ 23.2%
SD-15%	12	STONE	35.31 $\pm$ 0.46	52.87 $\pm$ 0.57	34.05 $\pm$ 1.73	43.65 $\pm$ 0.85	66.07 $\pm$ 1.28	30.47 $\pm$ 1.40
		w/ ST-TTC	34.86 $\pm$ 0.15	52.25 $\pm$ 0.54	29.80 $\pm$ 0.79	41.93 $\pm$ 0.62	63.17 $\pm$ 0.29	27.70 $\pm$ 0.03
		$\Delta$	$\downarrow$ 1.3%	$\downarrow$ 1.2%	$\downarrow$ 12.5%	$\downarrow$ 3.9%	$\downarrow$ 4.4%	$\downarrow$ 9.1%
	Avg.	STONE	28.45 $\pm$ 0.05	41.30 $\pm$ 0.26	36.02 $\pm$ 2.91	33.20 $\pm$ 0.69	49.19 $\pm$ 0.97	29.77 $\pm$ 3.00
		w/ ST-TTC	26.59 $\pm$ 0.22	39.90 $\pm$ 0.09	24.96 $\pm$ 1.00	30.65 $\pm$ 0.29	46.24 $\pm$ 0.52	22.50 $\pm$ 0.38
		$\Delta$	$\downarrow$ 6.5%	$\downarrow$ 3.4%	$\downarrow$ 30.7%	$\downarrow$ 7.7%	$\downarrow$ 6.0%	$\downarrow$ 24.4%
SD-20%	12	STONE	36.13 $\pm$ 0.76	53.87 $\pm$ 0.44	34.19 $\pm$ 1.08	41.64 $\pm$ 1.23	63.19 $\pm$ 2.11	37.38 $\pm$ 3.29
		w/ ST-TTC	35.08 $\pm$ 1.08	52.37 $\pm$ 0.67	30.55 $\pm$ 1.13	40.10 $\pm$ 1.41	60.77 $\pm$ 2.07	33.70 $\pm$ 2.73
		$\Delta$	$\downarrow$ 2.9%	$\downarrow$ 2.8%	$\downarrow$ 10.6%	$\downarrow$ 3.7%	$\downarrow$ 3.8%	$\downarrow$ 9.8%
	Avg.	STONE	28.86 $\pm$ 0.13	41.72 $\pm$ 0.14	34.89 $\pm$ 1.15	31.46 $\pm$ 0.95	46.06 $\pm$ 1.60	36.35 $\pm$ 4.23
		w/ ST-TTC	26.67 $\pm$ 0.29	39.71 $\pm$ 0.08	24.92 $\pm$ 0.81	28.94 $\pm$ 0.79	43.29 $\pm$ 1.32	26.60 $\pm$ 2.49
		$\Delta$	$\downarrow$ 7.6%	$\downarrow$ 4.8%	$\downarrow$ 28.6%	$\downarrow$ 8.0%	$\downarrow$ 6.0%	$\downarrow$ 26.8%

## F More Discussion

### F.1 Distinction between Spatio-Temporal Forecasting and Long-Term Time Series

As stated in the paper, our work adheres to the common settings of previous short-term and long-term spatio-temporal forecasting studies (*e.g.*, 12  $\rightarrow$  12, 24  $\rightarrow$  24) (Shao et al., 2022a, 2024b). However, we are fully aware of the 96  $\rightarrow$  96  $\rightarrow$  720 settings prevalent in current long-term time series forecasting. We wish to share our insights regarding this:

- ❶ There has been a long-standing debate concerning the long-term predictability of time series (Bergmeir, 2024; Brigato et al., 2025), which we do not intend to overly critique here. Nevertheless, it is important to note that in spatio-temporal forecasting, specifically in traffic flow theory research, previous studies (Zheng et al., 2025) utilizing residual analysis have indicated that, after minimizing periodicity, the correlation between traffic data beyond one hour and the past hour’s observations is significantly limited for most sensors. Furthermore, typical traffic sensor data collection frequency is approximately 5 minutes. Therefore, for practical traffic forecasting and decision-making scenarios, which usually focus on the next 1-2 hours (*i.e.*, max 24 steps), our settings are more aligned with real-world applications.
- ❷ Given that spatio-temporal forecasting can be considered a complex extension of time series forecasting, the additional dimension of sensor count (up to hundreds or thousands) results in an order of magnitude higher data training cost. This is a secondary reason why existing spatio-temporal forecasting often considers 12-step settings.
- ❸ Another notable finding is that a recent study on the accuracy law of deep time series forecasting (Wang et al., 2025b), emerging subsequent to this paper, identifies a significant exponential relationship between the minimum prediction error of current deep forecasting models and the complexity of window series patterns. Adopting a Spectral-domain perspective similar to that of this paper, it defines the complexity of series patterns as the total variance of the amplitude spectrum distribution, thereby characterizing the intrinsic heterogeneity of series variations within each relevant window. This approach aligns with ours and provides a novel perspective to explain the learnability and effectiveness of the single-step gradient descent in our

calibrator. While the study focuses solely on univariate time series forecasting, this limitation does not inherently undermine its relevance. It is worth noting that the study concludes that mainstream time series models have not yet reached saturation on traffic scenario-based benchmarks. However, we hold a different view, arguing that this conclusion primarily stems from the study’s exclusive use of time series forecasting models, while neglecting mainstream spatio-temporal dependency modeling models. For further in-depth discussions, we suggest that future research should address this aspect.

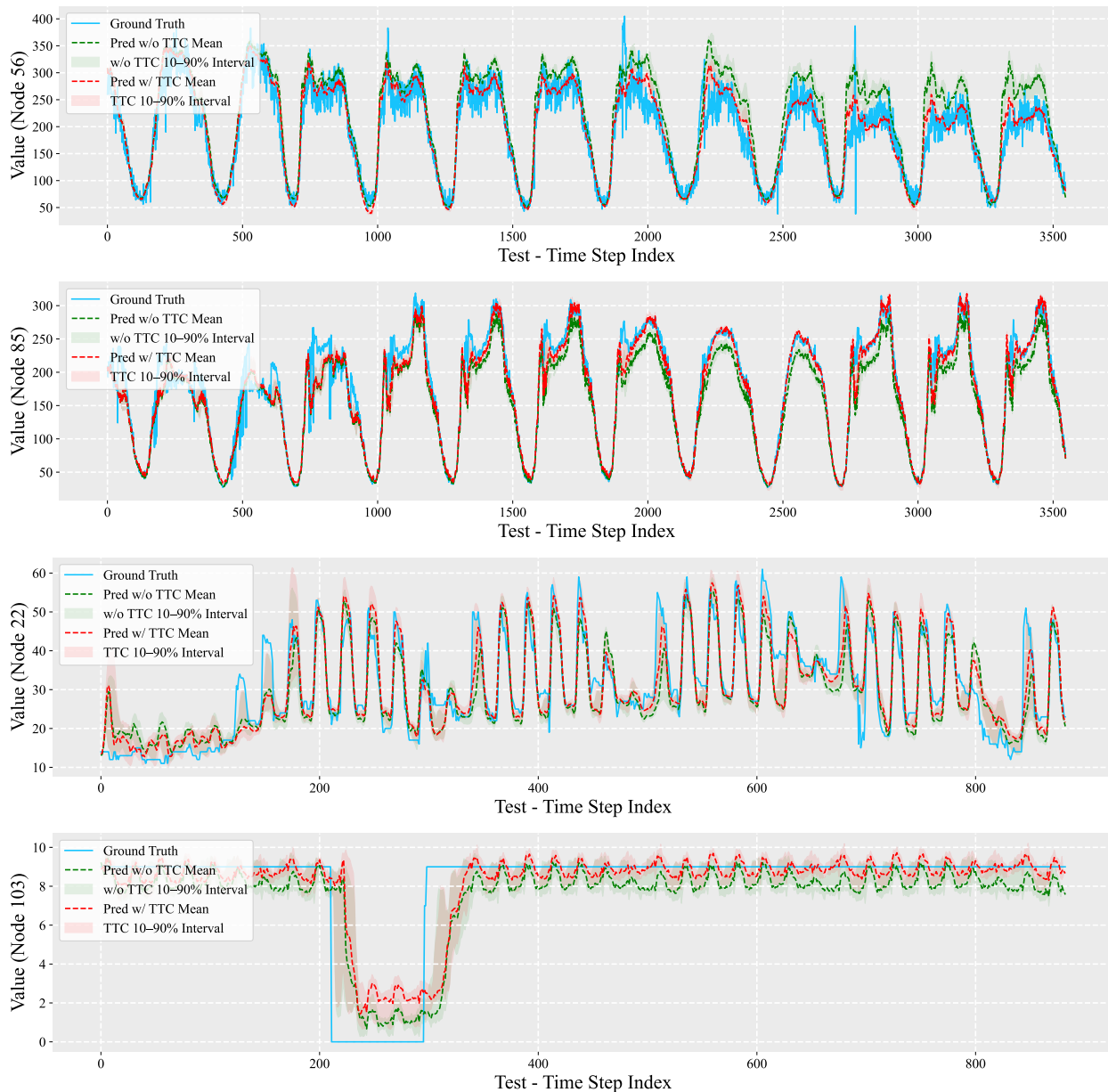


**Figure F.1** Show case of improvement in spatio-temporal forecasting through our ST-TTC .

## F.2 Limitation

In this paper, we propose a novel paradigm for spatio-temporal forecasting: test-time computing. Although there are still many potential areas for improvement, given the superiority and generality of our ST-TTC , we believe this provides a pathway for future exploration of larger-scale and more effective test-time computation. While we have taken a small step in this direction, several limitations warrant attention:

❶ Our current study does not involve testing on spatio-temporal foundation models. The fundamental reason behind this is our belief that true spatio-temporal foundation models do not yet exist. Although some preliminary exploratory work has been done (Yuan et al., 2024a,b; Li et al., 2024a,c; Yu et al., 2024), they are far from achieving true zero-shot generalization. However, considering their future inevitability, we believe that further improving the paradigm of test-time computation, especially how to activate and scale the internal capabilities of spatio-temporal foundation models during testing, goes beyond the design philosophy of our proposed learning with calibration. Nevertheless, our experiments still provide some preliminary guidance and insights.

❷ It is undoubtedly encouraging that our current calibration mechanism is more effective in large-scale and out-of-distribution scenarios. However, for commonly used small spatio-temporal benchmark datasets, the performance improvement is not yet significant. Therefore, how to effectively improve the performance of test-time computation on small-scale spatio-temporal datasets still requires exploration, and we reserve further improvement efforts for future research.

❸ We observed in our experiments that utilizing a larger amount of test information that is more similar to the current test sample does not significantly affect the results. This is certainly beneficial for real-time efficiency requirements. However, considering our current efficiency is already sufficiently good, further exploration is needed on how to potentially slow down the test-time computing process to make it more scalable and improve forecasting effectiveness.

### F.3 Future Work

Building upon the research direction presented in this paper, we envision future work encompassing two main aspects:

❶ Exploring how to integrate retrieval-augmented techniques to filter more effective learning samples from arbitrary external scenarios, thereby combining them with our test-time computation framework to optimize performance on small-scale datasets.

❷ Investigating the construction of real spatio-temporal foundation models that encapsulate internal compressed knowledge, and exploring how to activate this internal capability during test time.

## G Broader Impacts

This paper aims to promote the real-world usability of spatio-temporal forecasting models. We propose a novel paradigm, namely test-time computing of spatio-temporal forecasting. This paradigm shows significant generalization, universality across multiple scenarios, multiple tasks, multiple learning paradigms, and scalability to improve performance, providing valuable insights for future research and application value for practitioners. This paper focuses mainly on scientific research and has no obvious negative impact on society.